CHAPTER-VI

Modelling of Potato Late Blight Disease using Multispectral Multi-temporal Satellite Data

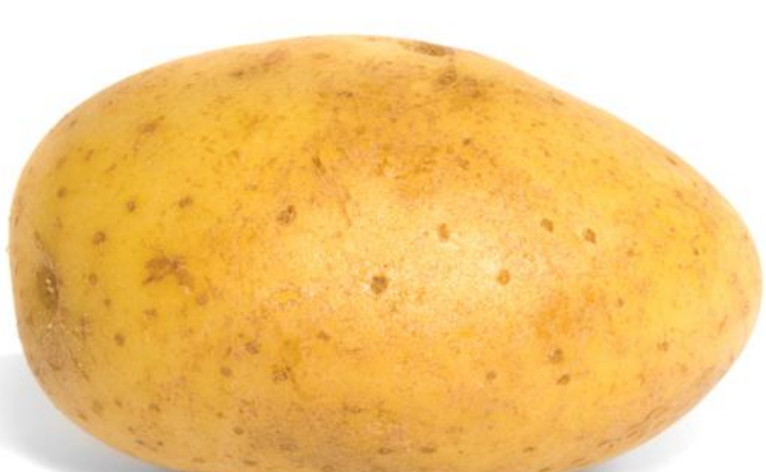

MODELLING OF POTATO LATE BLIGHT DISEASE USING MULTISPECTRAL MULTI-TEMPORAL SATELLITE DATA

6.1 Introduction

Potato is a major food crop after wheat, rice and maize in the world. Extensive old and recent alluvium of the Indo-Gangetic region is ideal for potato cultivation during winter season. The area and production of potato has increased from 18.63 lakh ha to 19.92 lakh ha and 42.34 million tons to 45.34 million tons during 2010-11 and 2012-13 (http://nhm.nic.in). However, the crop suffers from many pests and diseases among which the notable one is late blight, caused by the Oomycete of *Phytophthora infestans*. The potato blight causes havoc under favourable weather condition. In India, late blight occurs every year in north-western hills of Himachal Pradesh, Uttarakhand, North-Eastern hills of Meghalaya and the South Indian hills. In the initial stages of potato late blight large brown to purplish black necrotic spots appears on the leaves which develop fast and kill the entire foliage within few days. The disease spreads quickly in potato fields under suitable weather conditions during growing season (Wisler et al., 2000). In potato growing regions of West Bengal late blight appears normally between 2^{nd} to 3^{rd} week of January under optimum environmental condition as defined by temperature range of 12.8 to 21.7^{0}C, relative humidity 65 to 98%, sunshine hours 0.5 and rainfall amount 5.6–6.3 mm up to 7 days prior to onset of the disease (Basu et al., 2009). Prolonged cloud cover with light rain is the most congenial situation for potato blight during the 2^{nd} half of January. Apart from ambient weather condition farm management practices such as irrigation and crop management practices also contribute to the potential risk of the disease in some potato fields (Zhang et al., 2004). Presently, potato growers of West Bengal are incurring huge financial loss due to routine application of pesticides as preventive measure to keep the disease at bay. The indiscriminate use of pesticides is also a great concern for the environmental safety.

Traditionally, the assessment of disease affected areas are carried out by field scouting which is time consuming, labour intensive and inadequate for adopting timely intervention through field spraying. Hence, there is a need to develop alternate method which can complement traditional methods and collect synoptic information at regular temporal interval. A rapid, reliable and non-invasive approach of disease detection from a vantage point offers valuable quantitative and near real time information about crop health and disease progress. Earth observation satellites have the advantage to capture the anomaly in crop bio-optical characteristics and monitoring at acceptable temporal scale. The spectral reflectance of canopy was found to be capable of detecting pathogen-induced biophysical changes in the plant. Diseased crops differ in the absorption of solar energy in the visible and NIR range while comparing with healthy crops (Carter and Knapp, 2001; Adams et al., 1999; Dawson and Curran, 1998; Lichtenthaler et al., 1996; Gitelson and Merzlyak, 1996; Guenther, 1990). In general, disease affected plants show higher reflectance in the red and lower in the NIR region depending on the infection severity. This altered response could be due to the combined effect of decreased chlorophyll content, and the change in internal structure of the leaves. Due to PLB disease the crop leaves structure get damaged and chlorophyll concentration get decreased. As a result, red absorption decrease and reflectance increase in red reflectance. On the other hand, as crop leaves spongy cell tissue structure get damaged, multiple internal reflectance decrease in NIR band. As a result NDVI value was decreased after PLB disease infestation (Ray et al., 2011). Several studies have been carried out on the relationship between chlorophyll content and spectral reflectance in visible and NIR regions (Carter et al., 1996; Gitelson and Merzlyak, 1996; Datt, 1999; Blackburn and Steele, 1999). Zhang et al. (2002) have shown that NIR is much more useful than visible region for detecting stress in late blight affected tomatoes. Like visible and NIR region water absorption bands in the shortwave infrared region also respond to changes in leaf water content in the diseased canopies by increasing the reflectance. Apan et al. (2004) studied the role of the SWIR bands in the discrimination of healthy and diseased (orange rust) sugarcane crop. The detection of stress induced by late blight disease in tomato have been studied by Zhang et al. (2003) who has shown decreased spectral reflectance in the NIR caused by the changes of internal structure of diseased plants. The possibility of detecting pests and diseases by optical sensors, onboard aircraft or satellites, has attracted lot of interest in recent years as satellite based methods have potential in scouting for disease or pest damage over large areas which are difficult to survey or inaccessible.

Several vegetation indices using broadband and narrowband spectral data have been developed to detect plant stress and disease (Carter et al., 1996). Vegetation indices are able to overcome the environmental effects and hence, relate well with plant biochemical constituents (Delalieux et al., 2009). Different spectral band combinations have been identified by various researchers to detect plant stress and diseases. The Normalized Difference Vegetation Index (NDVI) is very sensitive to the changes of chlorophyll content and leaf structure which has been widely used for crop growth monitoring and detection of disease infected crop canopy. Dutta et al. (2014) studied the spectral response of healthy and late blight affected potato crops using NDVI and land surface water index (LSWI). They have shown a large difference between their profiles. Vegetation indices are also widely used to monitor green vegetation fraction (GVF) which is an important morphological property of plant canopy (Xiao Bing et al., 2003) and can serve as proximal indicator for canopy density. This is considered to be one of the important input parameter for assessment of disease vulnerability.

To assess the disease spread within a limited temporal window satellite data of high temporal revisit is a prerequisite. Advance Wide Field Sensor (AWiFS) onboard Indian remote sensing satellite Resourcesat-2 (56 m spatial resolution) is ideal for spatio-temporal mapping and analysis of disease geography due to its wide swath, moderate spatial resolution, better temporal revisit (5 days) and availability of required spectral bands.

The aim of the present research is to i) evaluate the efficiency of multi-temporal NDVI and shortwave angle based indices derived from AWiFS data in identifying canopy pigment and moisture anomaly that might be associated with potato late blight disease ii) to distinguish the disease affected potato crops from the healthy ones by using remote sensing based indices and iii) use of multi-spectral data in hindcast model of late blight disease towards disease detection.

6.2 Objectives

The main objectives of this study is in the following,

- To evaluate the utility of multispectral vegetation indices to distinguish the disease affected potato crops and risk mapping.
- To develop potato late blight disease monitoring method using multispectral remote sensing data and mapping of disease severity.

6.3 Materials And Methods

6.3.1 Data Used

In the present study, multi-temporal cloud free AWiFS data (Table 6.1) of onboard Resourcesat-2 satellite were used. The AWiFS sensor acquires information through four spectral bands (Green 0.52–0.59 μm), Red (0.62–0.68 μm), NIR (0.77–0.86 μm), and SWIR (1.55–1.70 μm) with ground swath of 740 km spatial resolution of 56 m. Resourcesat-2 is a polar orbiting satellite with 10 bits radiometric resolution and has five days temporal resolution. The cloud free AWiFS data were acquired for two successive potato growing season e.g. 2012-13 and 2013-14. In addition SOI toposheets(1:50,000 scale) and GPS (Garmin eTrex Legend Cx" twelve channel GPS receiver) was also used to collect field level information and location of PLB sightings.

Table 6.1: Details of the AWiFS Data Used for the Study

StudyYear	Path/Row	Date of Acquisition	Spatial Resolution	Swath	Spectral Bands
2012-13	105/55	December 22, 2012	56 m	740 Km	Green (0.52–0.59 μm)
	107/56	January 01, 2013			
	109/57	January 11, 2013			
	105/55	January 15, 2013			
	107/56	January 25, 2013			Red (0.62–0.68μm)
	109/57	February 04, 2013			
	108/57	February 23, 2013			
	109/57	February 28, 2013			
2013-14	105/55	December 17, 2013			NIR (0.77–0.86 μm)
	107/56	December 27, 2013			
	105/55	January 10, 2014			
	108/56	January 25, 2014			SWIR (1.55–1.70 μm)
	107/56	February 13, 2014			
	108/56	February 18, 2013			

6.3.2 Methodology

6.3.2.1 AWiFS Data Pre-processing

AWiFS datasets were registered with respect to Survey of India topomaps (1:50,000 scale) using 2nd order polynomial function and nearest neighbourhood resampling technique. Care was taken to keep the root mean square error less than one pixel. The AWiFS datasets were projected to UTM system with WGS84 datum. For radiometric correction, 'Top-of-atmosphere' (TOA) reflectance was calculated based on a physical model and calibration parameters of AWiFS sensor. The values of gain and offset were obtained from header information provided with each spectral band. The solar zenith angle and the earth-sun distance in astronomical unit was calculated and reflectance correction was applied for each band. The DN values were converted to radiance by using the following equation:

$$L_{\lambda} = \frac{(L_{max} - L_{min})}{Q_{cal\ max}} Q_{cal} + L_{min} \quad \text{.......................................} \quad (1)$$

Where,

L_{λ} = spectral radiance at the sensors aperture W/ (m^2.sr.µm)

Q_{cal} = calibrated Digital Number

Q_{calmax}= maximum possible DN value

L_{max}&L_{min} = scaled spectral radiance

TOA Reflectance value of the image pixel was calculated by using the following formula and possible atmospheric correction was applied to eliminate the atmospheric scattering or absorption by the atmospheric gases (water vapour and ozone) and aerosols.

$$\rho_{\lambda} = \frac{\pi L_{\lambda} D^2}{ESUN_{\lambda} \cos \theta_s} \quad \text{.......................................} (2)$$

Where,

ρ_{λ} = unitlessplantary reflectance

L_{λ}= spectral radiance (from equation 1)

D = Earth-Sun distance in astronomical units

$ESUN_{\lambda}$ = mean solar exoatmospheric irradiances

θ_s= solar zenith angle

6.3.2.2 Calculation of Spectral Vegetation Indices

Vegetation Indices derived from satellite data are one of the most valuable information for operational monitoring of plant health. Vegetation Indices are calculated by linear combination of spectrally sensitive bands, but most commonly red (R) and near infrared

(NIR) bands are used keeping their unique response to vegetation canopy. PLB disease severity was quantified using different vegetation indices.

6.3.2.2.1 Normalized Difference Vegetation Index

Normalized difference Vegetation Index (NDVI) is mostly used proximal indicator of crop vigour and health. It is related to both plant pigments and biophysical parameters. The NDVI is calculated by using the formula given by (Rouse et al., 1974):

$$NDVI = \frac{(R_{NIR} - R_{RED})}{(R_{NIR} + R_{RED})} \ldots\ldots\ldots\ldots\ldots\ldots (3)$$

Where, R_{NIR} and R_{RED} refers to spectral reflectance in near infrared and red region respectively. The values of NDVI range from -1 to +1. Band 2 and band 3 of AWiFS sensor are representative of red and infrared band.

6.3.2.2.2 Normalized Difference Water Index

Normalized Difference Water Index (NDWI) is sensitive to changes of canopy water stress and is less sensitive to atmospheric scattering than NDVI (Gao et al., 1996). The changes of canopy water content and the spongy mesophyll structure in crop canopies significantly affect the SWIR reflectance. It is presented as:

$$NDWI = \frac{(R_{NIR} - R_{SWIR})}{(R_{NIR} + R_{SWIR})} \ldots\ldots\ldots\ldots\ldots\ldots (4)$$

Where, R_{NIR} and R_{SWIR} are the spectral reflectance in NIR and SWIR, respectively. Band 4 and band 3 of AWiFS data were used for calculation of NDWI to obtain significant difference in the canopy water content between healthy and diseased crops. The NDWI values range from -1 to +1. High values of NDWI correspond to high canopy water content.

6.3.2.2.3 Angle Based Drought Index (ABDI)

The angle-based drought index (ABDI) was first conceptualized by Palacios-Orueta et al. (2006). The index examines the relationship between bands instead of absolute values of reflectance of the bands. An angle-based drought spectral index was aimed at drought monitoring based on Near Infrared (NIR, 858 nm) and Shortwave Infrared (SWIR, 1240 and 1640 nm) bands of the Moderate Resolution Imaging Spectrometer (MODIS). Khanna et al. (2007) proposed shortwave angle slope index (SASI) to estimate the surface moisture and discriminate land cover. In spite of its advantages, the SASI has remained under-utilized because of its requirement of two SWIR bands for computation. Due to non-availability of two SWIR bands in many of the medium resolution remote sensing sensors namely SPOT, AWiFS and NOAA AVHRR, the potential of the index was not fully utilized. A new angle-based drought index (ABDI) which parameterizes the shape of the broadband spectrum of the SWIR and NIR bands was proposed by Liu et al. (2010). Resoucesat-2 AWiFS data with single SWIR band was utilized to generate improved surface moisture information comparable to SASI at a better spatial resolution. ABDI index is defined as (Liu et al., 2010):

$$ABDI = R_{NIR} * tan^{-1}[\frac{R_{NIR} - R_{SWIR}}{slope}] \quad \text{……………………………} (5)$$

Where, slope =λ_{NIR}–λ_{SWIR}, R_{NIR} and R_{SWIR} are the spectral reflectance in NIR and SWIR region respectively. For vegetation, the value of ABDI is positive, with high value for green vegetation in comparison to dry vegetation. For soils, the value of ABDI is negative, wherein dry soil is having lower value than that of wet soil (Liu et al., 2010).

6.3.2.2.4 Potato Crop Canopy Fraction (PCCF) Estimation using Dimidiate Pixel Model (DPM)

Potato crop canopy fraction (PCCF) refers to the percent of the vertical projection of green vegetation cover of the potato crop including leaves, stem and branches in the total statistical area of land surface (Bonham, 1989; Purevdorj et al., 1998; Gitelson et al, 2002; Godinez-Alvarez et al., 2009 and Jing et al., 2010). It constitutes an important plant canopy morphological property (Xiao-Bing et al., 2013) and plays a crucial role in energy and moisture exchange across the earth’s surface and atmosphere. The index is a sensitive bio-indicator for identifying vegetation anomalies. One of the method of estimation of PCCF is Dimidiate Pixel Model (Cui et al., 2010). It is based on spectral mixture analysis that assumes spectral signal received from a ground pixel is the sum of the fractional abundance of pure soil and pure vegetation in the mixed pixel, the contribution by vegetation in the mixed pixel is expressed as:

$$S = f_c \times S_{veg} + (1 - f_c)S_{soil} \quad \text{...(6)}$$

Where, 'f_c' is the vegetation fraction, '(1- f_c)' is the soil fraction, 'S_{veg}' is the signal of a pure vegetation pixel, and 'S_{soil}' is the signal of a pure soil pixel. Equation 6 can be rewritten as:

$$f_c = \frac{(S - S_{soil})}{(S_{veg} - S_{soil})} \quad \text{.. (7)}$$

The major advantage of the dimidiate pixel model is that the impacts from atmosphere, soil background and vegetation types are reduced (Zhang et al., 2012). Using NDVI as approximation of vegetation fraction equation 7 can further be rewritten as,

$$f_c = \frac{NDVI - NDVI_{soil}}{NDVI_{crop\_canopy} - NDVI_{soil}} \quad \text{.. (8)}$$

Where $NDVI_{soil}$ represents the soil NDVI with no vegetation cover and $NDVI_{Crop\_canopy}$ represents the maximum NDVI value in the data set. In the present study the values of $NDVI_{Crop\_canopy}$ and $NDVI_{soil}$ are computed to be 0.62 and 0.07 respectively.

6.3.2.3 Field Measurement of Potato Late Blight Disease Severity

During the field visit visual assessment of potato late blight disease severity was estimated and grouped into nine classes (0-8) according to the disease rating scale described by James et al. (1947) where, 0 = healthy/no lesions, 1 = up to 0.1% (few scattered plants blighted with 1 or 2 spots), 2 = 1% (seen upto 10 spots per plant or general light infection), 3 = 5% (up to 50 spots per plant, 1 to10 leaflets infected), 4 = 25% (nearly every leaflet is infected, field looks green although every plant is affected), 5 = 50% (every plant is affected and about 50% of leaf area is destroyed; field appears green but flecked with brown), 6 = 75% (about 75% of leaf area is destroyed; field appears neither predominantly brown nor green), 7 = 95% (only few leaves remained on the plants, but stems are green) and 8 = 100% (all leaves are dead, stems are dead or dying) affected. Due to scalability issue and large footprint of satellite data field based disease severity assessment was done using stratified approach. In which the large contiguous patches of potato fields having similar types of disease severity were selected. Within each strata several field observations were made to mimic the coarse footprint of AWiFS pixel.

6.3.2.4 Segregation of Potato Crop Pixels

A rule based classification technique was adopted based upon the temporal spectral profile, field intelligence and ancillary data to segregate the potato crop pixels from the image. Classification was done using atmospherically corrected AWiFS scenes in ERDAS Imagine (ver. 9.0) image processing software to pick up the particular potato crop pixel from other crops as well as non-cropped areas. According to their spectral profile AWiFS scenes were clustered into fifty classes. Potato crop pixels were picked up from those clusters based on field knowledge and ground truth data points of potato crops.

6.3.2.5 Field Validation

To check the classification accuracy field information was collected using hand held GPS from both healthy and diseased potato fields during a field campaign on 2nd February, 3rd February and 21st February of 2013 and 21st January, 25th January, 5th February and 9th February of 2014. In the field *Phytophthora infestans* is characterized by large brown to purplish black necrotic spots in large patches. To compensate for the scale mismatch between location based GPS observation and satellite footprint, the area was divided into 56 m grid and field observations were collected from 5 different locations within each grid which were then averaged for upscaling. The field data were grouped into two e.g. i) for generation of rule / model and ii) for validation.

6.3.2.6 Estimation of Model Accuracy

To compare the predictive ability of the satellite derived disease severity index in relation to field measured disease severity statistical performance indicators such as coefficient of determination (R^2), root mean square error (RMSE), relative RMSE, D-index, coefficient of residual mass (CRM) and modeling efficiency (ME) were used which is defined as:

$$RMSE = \sqrt{\frac{1}{n}\sum_{i=1}^{n}\left(P_i - O_i\right)^2} \quad \ldots\ldots (9)$$

$$Relative\,RMSE = \frac{1}{\bar{O}}\sqrt{\frac{1}{n}\sum_{i=1}^{n}\left(P_i - O_i\right)^2} \quad \ldots\ldots (10)$$

$$CRM = \left(\frac{\sum_{i=1}^{n} O_i - \sum_{i=1}^{n} P_i}{\sum_{i=1}^{n} O_i}\right) \quad \ldots\ldots (11)$$

$$D - index = 1 - \left[\frac{\sum_{i=1}^{n}(P_i - O_i)^2}{\sum_{i=1}^{n}\left(P'_i + O'_i\right)^2}\right] \quad \ldots\ldots (12)$$

$$ME = 1 - \left[\frac{\sum_{i=1}^{n}(P_i - O_i)^2}{\sum_{i=1}^{n}(P_i - \bar{O})^2}\right] \quad \ldots\ldots (13)$$

Where, P_i= predicted value

O_i= measured value

$\bar{O}$ = measured mean value

$P'_i = P_i - \bar{O}$

$O'_i = O_i - \bar{O}$

n = number of observations

These statistics have been widely used for model evaluation. The RMSE value represents the absolute deviation of predicted and measured value of a model. The coefficient of resudial mass (CRM) indicates the overall under- or over-estimations in case of the +ve values and –ve values respectively. For a perfect match, the CRM value is zero. To make cross-comparisons in between predicted and measured values D-index is used. The ME is sensitive to extreme values and might yield sub-optimal results when the dataset contains large outliers. For a perfect prediction, the ME value would be one. The ME value close to one indicates more accurate model. The details can be found in Willmott (1982) and Kobayashi and Salam (2000).

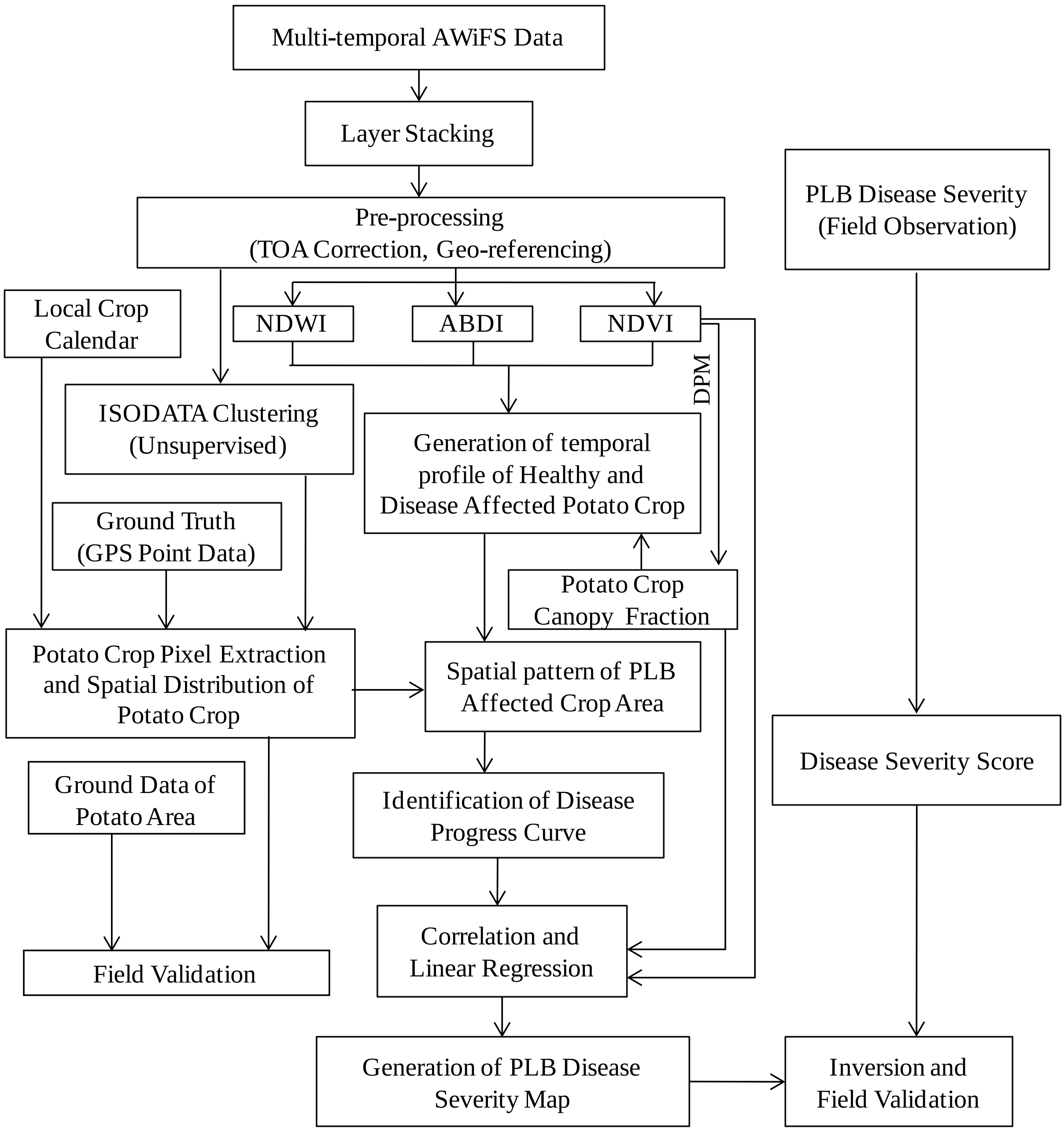

Figure 6.1: Overall Methodology for Multispectral Data Processing

6.4 Result And Discussion

6.4.1 Spectral Reflectance of Diseased and Healthy Potato Crops

The canopy reflectance derived for different bands of AWiFS satellite data from healthy and PLB infested canopy for the year 2012-13 and 2013-14 are presented in table 6.2 and table 6.3. It was apparent that disease plants have higher reflectance in red region and lower reflectance in NIR region compared to healthy plants. The higher value of reflectance in red band might be due to the combined effect of decreased chlorophyll synthesis and browning of leaves whereas decreased reflectance in NIR region could be due to damage of internal leaf structure and desiccation. Higher values in SWIR band reflectance might be due to decrease of water content in plant canopy.

Table 6.2: Reflectance of AWiFS Bands for Healthy and Diseased Plants at Consecutive Dates of Satellite Overpass During 2012-13 Crop Season

PLB Incidence	25th Jan 13			04th Feb 13			% Change in R_{RED}	% Change in R_{NIR}	% Change in R_{SWIR}
	R_{RED}	R_{NIR}	R_{SWIR}	R_{RED}	R_{NIR}	R_{SWIR}			
Healthy Crop									
1	0.48	1.82	0.66	0.46	1.86	0.66	-2.92	2.13	-1.07
2	0.46	1.60	0.61	0.41	1.65	0.60	-13.77	3.11	-1.66
3	0.42	1.55	0.58	0.40	1.59	0.56	-5.10	2.13	-2.77
4	0.43	1.58	0.59	0.41	1.64	0.58	-6.17	3.66	-1.72
Average	0.45	1.64	0.61	0.42	1.69	0.60	-6.99	2.76	-1.81
Diseased Crop									
1	0.45	1.30	0.83	0.54	0.90	0.86	16.91	-43.90	3.81
2	0.50	1.24	0.88	0.53	0.98	0.93	5.50	-26.01	5.51
3	0.49	1.25	0.86	0.53	0.95	0.89	8.20	-31.55	3.48
4	0.44	1.29	0.85	0.57	0.88	0.91	22.22	-46.94	6.55
5	0.36	1.34	0.78	0.53	0.93	0.85	30.79	-43.68	7.75
6	0.38	1.29	0.75	0.51	0.93	0.81	26.76	-38.44	7.76
7	0.41	1.33	0.76	0.54	0.99	0.85	24.08	-34.79	11.03
8	0.38	1.33	0.76	0.51	0.92	0.80	24.75	-44.74	4.61
Average	0.43	1.30	0.81	0.53	0.94	0.86	19.90	-38.76	6.31

Careful analysis of the change in spectral reflectance with advancement of phonological stages showed that in case of healthy plants there was slight decrease in Red and SWIR reflectance after the crop attained peak vegetative growth stage. At the same time, there was marginal increase in NIR reflectance. This might be due to the fact that the potato crops do not attain senescence and the leaves remain green while the tuber bulking continues for a considerable period of time.The tuber bulking stage is a very critical phase of potato growth when the photosynthesis process and the partitioning of photosynthates between aerial and underground part of the plant continues. On the other hand the PLB infested plants recorded abrupt decrease in NIR reflectance after it attained peak vegetative phase. This was an evidence of how potato late blight proliferates very fast after its onset. The rapid loss of leaf pigments, browning of leaves and development of necrotic spot followed by complete damage of leaves in quick succession could have led to abrupt drop in NIR reflectance.

Table 6.3: Reflectance of AWiFS Bands for Healthy and Diseased Plants at Consecutive Dates of Satellite Overpass During 2013-14 Crop Season

PLB Incidence	25th Jan 14			13th Feb 14			% Change in R_{RED}	% Change in R_{NIR}	% Change in R_{SWIR}
	R_{RED}	R_{NIR}	R_{SWIR}	R_{RED}	R_{NIR}	R_{SWIR}			
Healthy Crop									
1	0.47	1.77	0.59	0.45	1.82	0.55	-4.44	2.75	-7.27
2	0.44	1.59	0.57	0.39	1.65	0.51	-12.82	3.86	-11.76
3	0.41	1.55	0.63	0.39	1.68	0.59	-5.13	7.44	-6.78
4	0.43	1.67	0.64	0.41	1.72	0.60	-6.17	2.91	-6.67
Average	0.44	1.65	0.61	0.41	1.72	0.56	-7.14	4.24	-8.12
Diseased Crop									
1	0.42	1.28	0.81	0.52	0.91	0.88	19.23	-40.66	7.95
2	0.52	1.21	0.89	0.59	0.89	0.95	11.86	-35.96	6.32
3	0.48	1.24	0.85	0.54	0.93	0.93	11.11	-33.33	8.60
4	0.38	1.29	0.75	0.51	0.93	0.81	26.76	-38.44	7.76
5	0.38	1.33	0.76	0.51	0.92	0.80	24.75	-44.74	4.61
6	0.41	1.32	0.76	0.49	0.96	0.85	15.77	-37.50	11.03
7	0.36	1.39	0.79	0.52	0.91	0.86	29.81	-52.75	8.14
8	0.44	1.30	0.87	0.58	0.88	0.96	23.35	-47.81	9.38
Average	0.42	1.30	0.81	0.53	0.92	0.88	20.33	-41.40	7.97

6.4.2 Sensitivity Analysis of Vegetation Indices towards Discrimination of Diseased Crops from Healthy Crops

Sensitivity analysis is the study of how the uncertainty in the output of a mathematical model or system (numerical or otherwise) can be apportioned to different sources of uncertainty in its inputs (Saltellai, 2002; Saltellai et al., 2008). The present investigation is aimed at assessing the sensitivity of different spectral indices to the PLB infestation of potato. Various broad band spectral indices were calculated using time series AWiFS data to understand their capability to discriminate the disease affected potato crops.

6.4.2.1 Discrimination between Healthy and Diseased Crops on the Basis of NDVI

When a crop is infected by disease, the spectral reflectance in the blue, green, red and infrared region of the spectrum changes due to combined effect of plant pigment and leaf internal structure. The healthy plants reflects maximum in the green region, absorb red wavelengths and reflects the infrared radiation. Under stressed condition absorption is decreased in the visible and NIR reflectance also decreases. Theoretically NDVI can detect these subtle variations of bio-optical responses to diseased canopy.

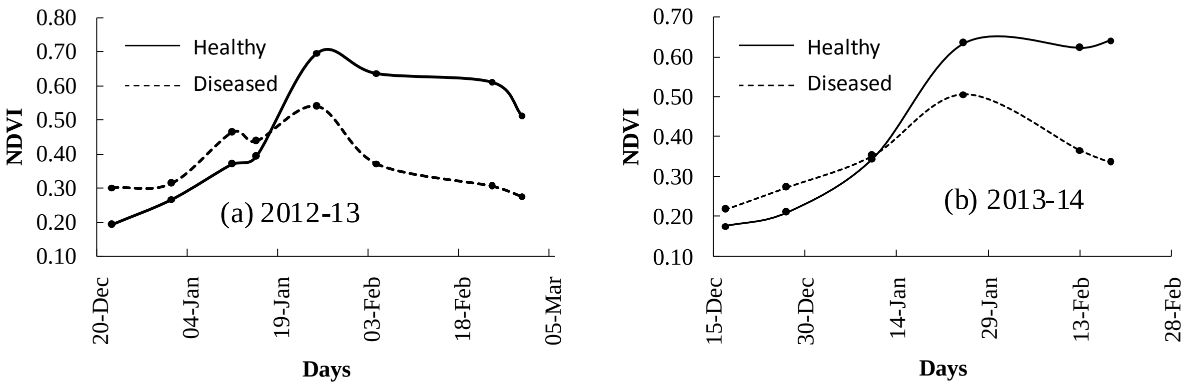

Figure 6.2: NDVI values of Diseased and Healthy Potato Canopy in (a) 2012-13 and (b) 2013-14

The NDVI profiles of healthy and diseased crops of both the years (2012-13 and 2013-14) are presented in Figure 6.2 (a) and 6.2 (b). It is apparent from the figure that NDVI of disease affected crop was generally higher than the healthy plants during initial growth phase in both the years. The NDVI of healthy crop stand recorded a steep increase after mid of January as the crop proceeds towards peak vegetative phase. But in case of diseased crop the NDVI increased at a slower rate. After peak vegetative stage (20^{th}-25^{th} January) the NDVI healthy crop showed a plateau or decreased very slowly as the crop continued with tuber bulking phase and then to maturity and gradual senescence of leaves, whereas in diseased plants the NDVI showed a sharp decrease in both the years.This change in NDVI due to late blight infestation was probably more due to pigment damage and necrosis than shortage of water supply.

The change in NDVI of healthy and disease affected crops in both the years (2012-13 and 2013-14) as presented in table 6.4 also implied that the NDVI of healthy plants remained almost at plateau with only 0.7 to 2% increase whereas during the same period the NDVI of the blight infested plants showed a negative growth. The decrease in NDVI was to the tune of 26 to as high as 41%.

Table 6.4: Changes of NDVI in Healthy and Diseased Crops

Location		NDVI (2012-13)			% Change
Latitude	**Longitude**	**15th Jan**	**25th Jan**	**04th Feb**	(25th Jan to 04th Feb)
Healthy Crop					
22° 57' 03.86"	88° 02' 37.13"	0.39	0.67	0.68	-1.22
22° 54' 14.97"	87° 57' 08.81"	0.40	0.64	0.65	-1.88
22° 50' 56.79"	87° 56' 50.09"	0.39	0.66	0.67	-2.25
Diseased Crop					
22° 50' 03.81"	87° 18' 47.81"	0.40	0.54	0.39	28.23
22° 55' 41.04"	87° 23' 07.11"	0.40	0.58	0.43	26.12
23° 17' 22.96"	87° 31' 39.24"	0.41	0.53	0.38	28.20
22° 57' 09.72"	87° 56' 51.60"	0.40	0.53	0.38	27.51
22° 39' 50.05"	86° 59' 57.60"	0.42	0.54	0.37	31.49
22° 50' 04.03"	87° 18' 43.74"	0.46	0.58	0.41	29.21
22° 49' 28.72"	87° 17' 56.18"	0.44	0.52	0.35	31.53
22° 31' 40.08"	87° 02' 34.08"	0.48	0.57	0.34	40.11
22° 43' 26.04"	87° 12' 25.02"	0.51	0.59	0.36	38.78
		NDVI (2013-14)			**% Change**
		10th Jan	**25th Jan**	**13th Feb**	(25th Jan to 13th Feb)
Healthy Crop					
23° 0' 20.45"	88° 13' 52.06"	0.34	0.66	0.67	-0.76
22° 55' 10.08"	87° 54' 19.59"	0.35	0.63	0.65	-1.94
22° 48' 19.23"	87° 52' 45.81"	0.34	0.64	0.65	-1.56
Diseased Crop					
22° 43' 26.40"	87° 12' 25.02"	0.36	0.53	0.39	26.48
22° 42' 07.20"	87° 04' 33.59"	0.33	0.61	0.43	29.46
22° 31' 40.08"	87° 02' 34.08"	0.38	0.41	0.31	26.15
22° 49' 28.72"	87° 17' 56.18"	0.29	0.47	0.28	41.15
22° 55' 41.04"	87° 23' 07.11"	0.30	0.53	0.37	30.52
23° 17' 22.96"	87° 31' 39.24"	0.34	0.53	0.39	26.65
22° 43' 19.20"	87° 12' 28.08"	0.31	0.48	0.32	34.37
22° 39' 50.05"	86° 59' 57.60"	0.44	0.47	0.34	27.81
22° 42' 07.20"	87° 04' 37.21"	0.43	0.56	0.37	34.64

The disease severity index and corresponding NDVI for PLB infested crops of all the districts under study were pooled and used fitting of appropriate regression curve. The analysis revealed that there was a strong negative correlation between NDVI and disease severity index (Figure 6.3) as implied by negative slope of the linear regression equation. The strength of relationship is demonstrated by high coefficient of regression of 0.837 in 2012-13 and 0.837 in 2013-14.

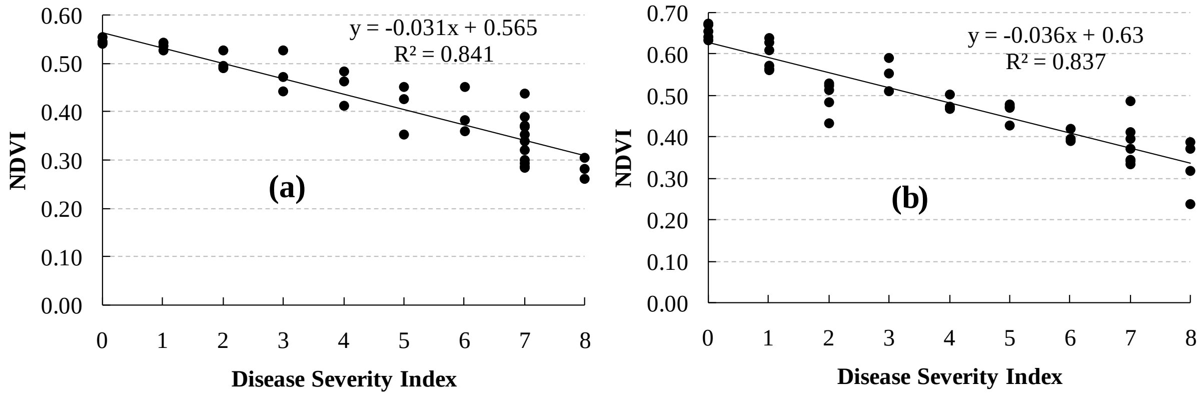

Figure 6.3: Relationship Between Disease Severity Index and NDVI in (a) 2012-13 and (b) 2013-14

6.4.2.2 Discrimination between Healthy and Diseased Crops on the Basis of NDWI

NDWI is very sensitive to changes in liquid water content of soil and vegetation, derived from SWIR and NIR bands. The index is used to monitor the changes in moisture content of plant due to water stress or disease infection. When potato crop is affected by late blight disease, leaf water content is affected resulting in reduced turgidity. As a result, hydroxyl absorption in the SWIR region is decreased.

Figure 6.4 shows NDWI profile of healthy and diseased affected potato crops of 2012-13 and 2013-14 cropping season. From the figure 6.4, it is apparent that NDWI profile of both healthy and diseased crops are followed almost the same phonological trends till mid of January 2013 and thereafter in figure 6.4(a) the NDWI profile of healthy crop is sharply increased due to peak vegetative growth stage. After peak vegetative growth stage (last week of January) the NDWI profile of healthy crop decreased very slowly due to tuber bulking phase and during maturity phase NDWI decrease rate slightly high due to senescence of leaves. The NDWI profile of healthy in figure 6.4(b) is gradually increased till 2^{nd} week of February and afterthat decreased similarly during maturity stage. In diseased affected crops the curve (figure 6.4(a)) abruptly falls after 25^{th} January 2013 and the same trend was followed after 25^{th} January 2014 in NDWI profile of 2013-14 (Figure 6.2(b)). As there was no shortfall of water, this change in NDWI indicate the unhealthy crop condition due to late blight infestation. Due to disease infestation, internal structure of leaves get damaged and reduces water flow in crop leaves. It is also worth noting that NDWI of disease affected crop was generally higher than the healthy plants during initial growth phase in both the years. As a result, high canopy density is creating the microclimate favourable for the pathogen. But after disease infection it decreases sharply.

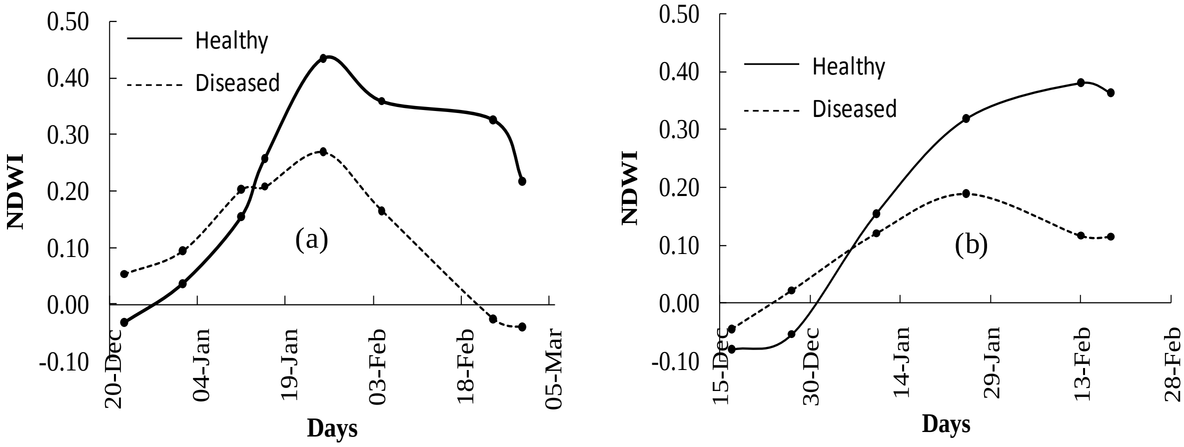

Figure 6.4: NDWI Values of Diseased and Healthy Potato Canopy in (a) 2012-13 and (b) 2013-14

The percentage change of NDWI in diseased and healthy crops in both the years (2012-13 and 2013-14) as presented in table 6.5 also implicit that the NDWI of healthy plants remained almost at plateau with only 2% to 5% increase whereas during the same period the NDWI of the late blight infested plants showed a negative growth with the decrease values of NDWI was to the tune of 27% to as high as 86%.

Table 6.5: Changes of NDWI in Healthy and Disease Crops

Location		**NDWI (2012-13)**			**% Change**
Latitude	**Longitude**	**15th Jan**	**25th Jan**	**04th Feb**	(25th Jan to 04th Feb)
Healthy Crop					
22° 57' 03.86"	88° 02' 37.13"	0.28	0.45	0.46	-2.88
22° 54' 14.97"	87° 57' 08.81"	0.23	0.42	0.43	-2.38
22° 50' 56.79"	87° 56' 50.09"	0.26	0.43	0.45	-3.56
Diseased Crop					
22° 50' 03.81"	87° 18' 47.81"	0.16	0.28	0.19	32.62
22° 55' 41.04"	87° 23' 07.11"	0.17	0.32	0.22	29.21
23° 17' 22.96"	87° 31' 39.24"	0.17	0.25	0.17	32.68
22° 57' 09.72"	87° 56' 51.60"	0.17	0.26	0.17	34.23
22° 39' 50.05"	86° 59' 57.60"	0.18	0.26	0.13	49.62
22° 50' 04.03"	87° 18' 43.74"	0.23	0.30	0.21	31.68
22° 49' 28.72"	87° 17' 56.18"	0.19	0.24	0.12	47.66

22° 31' 40.08"	87° 02' 34.08"	0.27	0.30	0.15	50.00
22° 43' 26.04"	87° 12' 25.02"	0.30	0.33	0.18	46.22
		NDWI (2013-14)			**% Change**
		10th Jan	**25th Jan**	**13th Feb**	(25th Jan to 13th Feb)
Healthy Crop					
23° 00' 20.45"	88° 13' 52.06"	0.14	0.39	0.40	-2.79
22° 55' 10.08"	87° 54' 19.59"	0.16	0.40	0.42	-5.25
22° 48' 19.23"	87° 52' 45.81"	0.15	0.37	0.39	-5.41
Diseased Crop					
22° 43' 26.40"	87° 12' 25.02"	0.15	0.22	0.10	57.01
22° 42' 07.20"	87° 04' 33.59"	0.12	0.29	0.18	36.84
22° 31' 40.08"	87° 02' 34.08"	0.18	0.11	0.02	86.84
22° 49' 28.72"	87° 17' 56.18"	0.03	0.15	0.06	62.33
22° 55' 41.04"	87° 23' 07.11"	0.09	0.21	0.16	27.10
23° 17' 22.96"	87° 31' 39.24"	0.10	0.20	0.11	46.97
22° 43' 19.20"	87° 12' 28.08"	0.07	0.15	0.07	54.73
22° 39' 50.05"	86° 59' 57.60"	0.19	0.16	0.05	67.09
22° 42' 07.20"	87° 04' 37.21"	0.18	0.24	0.08	67.37

NDWI values of PLB disease infested crops and respective disease severity index of all the districts under study were gathered and used fitting of appropriate regression curve. The analysis showed a strong negative correlation between NDWI and disease severity index (Figure 6.5) as implied by negative slope of the linear regression equation. The coefficient of determination (R^2) of NDWI was found to be 0.761 in 2012-13 whereas in 2013-14 it was found to be 0.744.

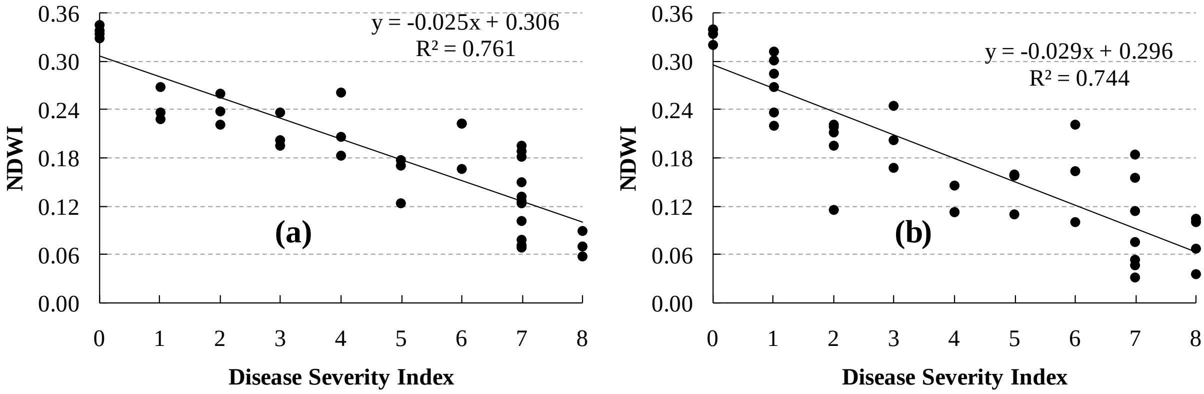

Figure 6.5: Relationship Between Disease Severity Index and NDWI in (a) 2012-13 and (b) 2013-14

6.4.2.3 Discrimination between Healthy and Diseased Crops on the Basis of ABDI

ABDI values primarily depend on moisture content of crop leaves and the reflectivity of SWIR is greatly affected by the canopy water content. ABDI was calculated from time series AWiFS dataset where positive values represents green healthy canopy and negative values represents the dry non-photosynthetic vegetation.

The ABDI profiles of healthy and diseased crops of both the years (2012-13 and 2013-14) are presented in Figure 6.6 (a) and 6.6 (b). It is observed from the figure that ABDI of disease affected crop was generally higher than the healthy plants during initial growth phase in both the years. The ABDI of healthy crop is increased sharply after mid of January due to the abundance of canopy water of potato canopy as the crop proceeds towards peak vegetative phase. But in case of diseased crop the ABDI increased at a slower rate. After peak vegetative stage the ABDI of healthy crop decreased very slowly similar to NDWI, whereas in diseased plants the ABDI showed a sharp decrease in both the years. The abruptly fall of ABDI due to PLB infestation was probably more due to decrease of water content of crop canopy in PLB disease affected dry non-photosynthetic vegetation.

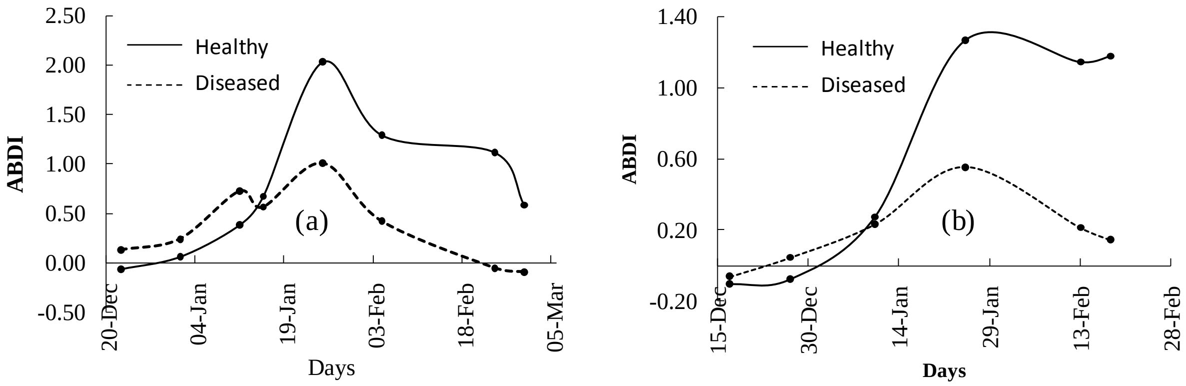

Figure 6.6: ABDI Values of Diseased and Healthy Potato Canopy in (a) 2012-13 and (b) 2013-14

The percentage change of ABDI values in healthy and disease affected crops in both the years (2012-13 and 2013-14) is presented in table 6.6. From the table 6.6 it is observed that ABDI of healthy plants remained almost at same with the increase values of 3% to 11% whereas during the same period the ABDI of PLB infested plants decreased 52% to as high as 91%.

Table 6.6: Changes of ABDI in Healthy and Diseased Crops

Location		ABDI (2012-13)			% Change
Latitude	**Longitude**	**15th Jan**	**25th Jan**	**04th Feb**	(25th Jan to 04th Feb)
Healthy Crop					
22° 57' 03.86"	88° 02' 37.13"	0.80	1.95	2.08	-6.41
22° 54' 14.97"	87° 57' 08.81"	0.54	2.01	2.09	-4.13
22° 50' 56.79"	87° 56' 50.09"	0.67	1.90	1.96	-3.03
Diseased Crop					
22° 50' 03.81"	87° 18' 47.81"	0.37	1.11	0.50	54.86
22° 55' 41.04"	87° 23' 07.11"	0.36	1.29	0.61	53.02
23° 17' 22.96"	87° 31' 39.24"	0.36	0.88	0.40	53.88
22° 57' 09.72"	87° 56' 51.60"	0.39	0.88	0.42	52.27
22° 39' 50.05"	86° 59' 57.60"	0.44	1.08	0.36	66.27
22° 50' 04.03"	87° 18' 43.74"	0.62	1.27	0.57	54.86
22° 49' 28.72"	87° 17' 56.18"	0.52	0.90	0.32	64.69
22° 31' 40.08"	87° 02' 34.08"	0.82	1.10	0.35	68.31
22° 43' 26.04"	87° 12' 25.02"	1.03	1.34	0.43	67.73
		ABDI (2013-14)			**% Change**
		10th Jan	**25th Jan**	**13th Feb**	(25th Jan to 13th Feb)
Healthy Crop					
23° 00' 20.45"	88° 13' 52.06"	0.26	1.27	1.38	-8.87
22° 55' 10.08"	87° 54' 19.59"	0.29	1.26	1.40	-11.17
22° 48' 19.23"	87° 52' 45.81"	0.27	1.27	1.34	-6.07
Diseased Crop					
22° 43' 26.40"	87° 12' 25.02"	0.28	0.68	0.19	72.73
22° 42' 07.20"	87° 04' 33.59"	0.21	1.13	0.33	70.70
22° 31' 40.08"	87° 02' 34.08"	0.34	0.23	0.02	91.03
22° 49' 28.72"	87° 17' 56.18"	0.05	0.34	0.07	78.78
22° 55' 41.04"	87° 23' 07.11"	0.13	0.54	0.26	53.13
23° 17' 22.96"	87° 31' 39.24"	0.16	0.50	0.19	62.03
22° 43' 19.20"	87° 12' 28.08"	0.10	0.34	0.10	70.26
22° 39' 50.05"	86° 59' 57.60"	0.46	0.42	0.10	76.60
22° 42' 07.20"	87° 04' 37.21"	0.44	0.81	0.16	80.10

A regression analysis was done in between the disease severity index and corresponding ABDI values of late blight disease affected potato crops and found a strong negative correlation between ABDI and disease severity index (Figure 6.7). The strength of relationship is demonstrated by high coefficient of determination (R^2) of 0.801 in 2012-13 and 0.750 in 2013-14.

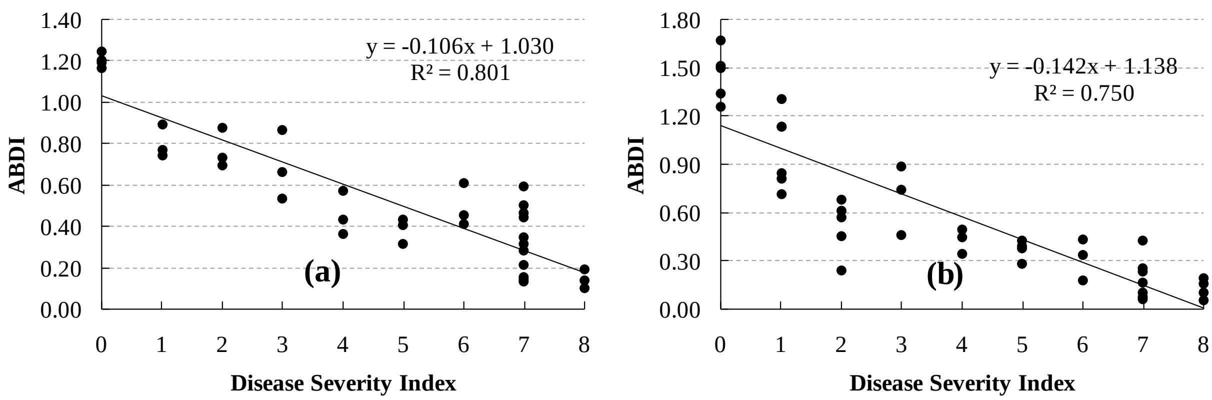

Figure 6.7: Relationship Between Disease Severity Index and ABDI in (a) 2012-13 and (b) 2013-14

6.4.2.4 Discrimination between Healthy and Diseased Crops on the Basis of PCCF

Potato canopy cover fraction (PCCF) is a measure of ground cover by the green photosynthetic vegetative crop which is sensitive to the chlorophyll content of crops. Dense vegetative crop cover shows high value in the NDVI whereas the areas with little or no vegetation shows very low or negative values. During full vegetative growth stage higher values of PCCF indicates complete canopy closure, which could be due to closer row to row distance leading to more disease susceptibility.

Figure 6.8 represents the potato canopy cover fraction of healthy and diseased crops of both the years (2012-13 and 2013-14). It is apparent from figure that all the diseased crops during initial growth phase had higher PCCF index values in both the years similar to above mention indices. It is noticeable that PCCF of both healthy and diseased crops are followed almost the same trends till mid of January and afterthat PCCF of healthy crop stand recorded a steep increase as the higher crop canopy closure during peak vegetative phase. But in case of diseased crop the PPCF after mid of January increased at a slower rate due to high canopy density created the microclimate favourable for the pathogen. After peak vegetative stage the PCCF of healthy crop decreased very slowly during maturity stage and gradual senescence of leaves, whereas in diseased plants the PCCF observed a sharp decrease in both the years. This change in PCCF to potato late blight disease infestation was probably more due to damage of foliage.

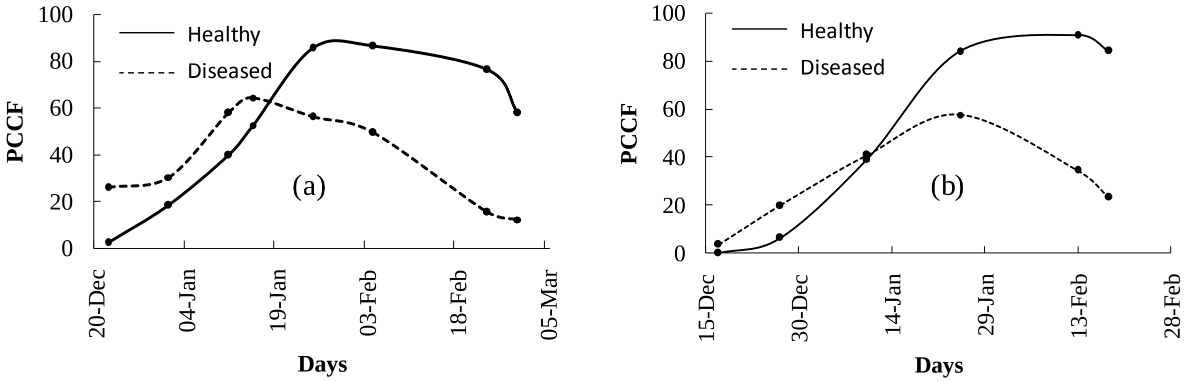

Figure 6.8: PCCF Values of Diseased and Healthy Potato Canopy in (a) 2012-13 and (b) 2013-14

In table 6.7 the changes of PCCF of healthy and disease affected crops in both the years (2012-13 and 2013-14) is presented and also observed that Similar like earlier observations, there is no significant change of the PCCF values of healthy plants and remained almost at plateau with only 0.4 to 7% increase whereas in PLB disease affected plants highly negative growth is found with the decrease values of 8% to as high as 35%.

Table 6.7: Changes of PCCF in Healthy and Diseased Crops

Location		**PCCF (2012-13)**			**% Change**
Latitude	**Longitude**	**15th Jan**	**25th Jan**	**04th Feb**	(25th Jan to 04th Feb)
Healthy Crop					
22° 57' 03.86"	88° 02' 37.13"	51.10	88.81	90.28	-1.48
22° 54' 14.97"	87° 57' 08.81"	54.02	82.19	82.63	-0.44
22° 50' 56.79"	87° 56' 50.09"	52.56	85.50	86.46	-0.96
Diseased Crop					
22° 50' 03.81"	87° 18' 47.81"	48.79	54.22	43.43	10.79
22° 55' 41.04"	87° 23' 07.11"	42.64	52.52	39.11	13.41
23° 17' 22.96"	87° 31' 39.24"	45.26	56.71	42.24	14.47
22° 57' 09.72"	87° 56' 51.60"	44.71	55.55	44.25	11.30
22° 39' 50.05"	86° 59' 57.60"	50.23	52.99	44.05	8.95
22° 50' 04.03"	87° 18' 43.74"	63.79	68.23	57.29	10.94
22° 49' 28.72"	87° 17' 56.18"	51.37	47.92	39.32	8.60
22° 31' 40.08"	87° 02' 34.08"	64.46	58.54	42.93	15.61
22° 43' 26.04"	87° 12' 25.02"	65.05	65.16	47.06	18.10
		PCCF (2013-14)			**% Change**
		10th Jan	**25th Jan**	**13th Feb**	(25th Jan to 13th Feb)
Healthy Crop					
23° 00' 20.45"	88° 13' 52.06"	37.90	83.74	91.14	-7.40
22° 55' 10.08"	87° 54' 19.59"	40.24	84.14	90.40	-6.26

22° 48' 19.23"	87° 52' 45.81"	39.07	83.94	90.77	-6.83
Diseased Crop					
22° 43' 26.40"	87° 12' 25.02"	42.22	61.49	38.82	22.67
22° 42' 07.20"	87° 04' 33.59"	36.02	79.32	48.65	30.67
22° 31' 40.08"	87° 02' 34.08"	48.72	38.58	20.97	17.61
22° 49' 28.72"	87° 17' 56.18"	25.03	49.98	14.73	35.25
22° 55' 41.04"	87° 23' 07.11"	27.56	63.42	35.45	27.97
23° 17' 22.96"	87° 31' 39.24"	38.36	62.40	39.29	23.10
22° 43' 19.20"	87° 12' 28.08"	29.87	53.00	23.56	29.44
22° 39' 50.05"	86° 59' 57.60"	61.89	50.42	28.79	21.63
22° 42' 07.20"	87° 04' 37.21"	59.56	69.41	34.91	34.51

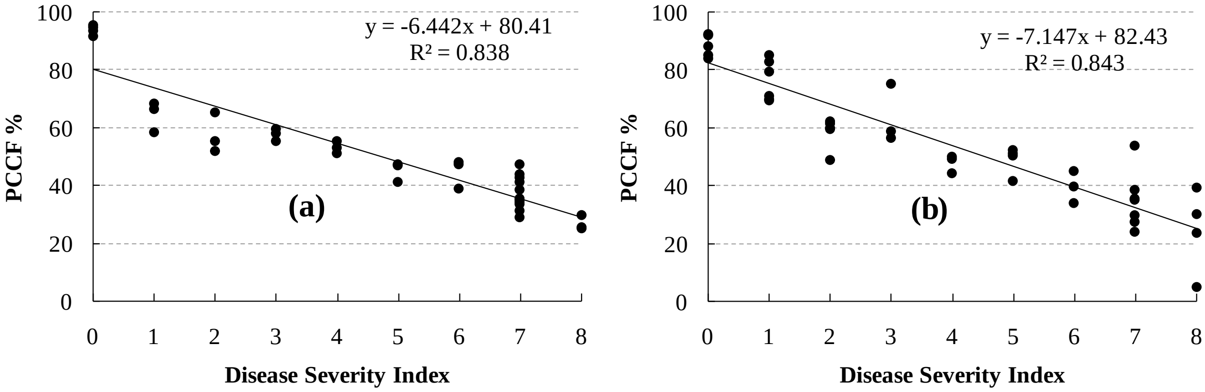

Figure 6.9: Relationship Between Disease Severity Index and PCCF in (a) 2012-13 and (b) 2013-14

Linear regression analysis among PCCF and late blight disease severity index were carried out by pooling all the data and used fitting of appropriate regression curve. As a result, significant negative correlation was found in between disease severity index and potato crop canopy fraction (Figure 6.9) as implied by negative slope of the linear regression equation. The R^2 values of PCCF and disease severity index was demonstrated to be 0.838 and 0.843 (figure 6.9) in the cropping season of 2012-13 and 2013-14 respectively.

6.4.3 Estimation of Late Blight Disease Affected Area

6.4.3.1 Visual Interpretation of Imageries

Visual analysis and comparison of AWiFS imageries of consecutive dates to have an initial idea of spatial progress of PLB disease in the study area. This approach is illustrated in Figure 6.10 using two dates satellite imageries (25.01.13 and 04.02.13) over Garhbeta-1 block. The informations obtained multidated satellite imageries was used formulate logic for rule based classification.

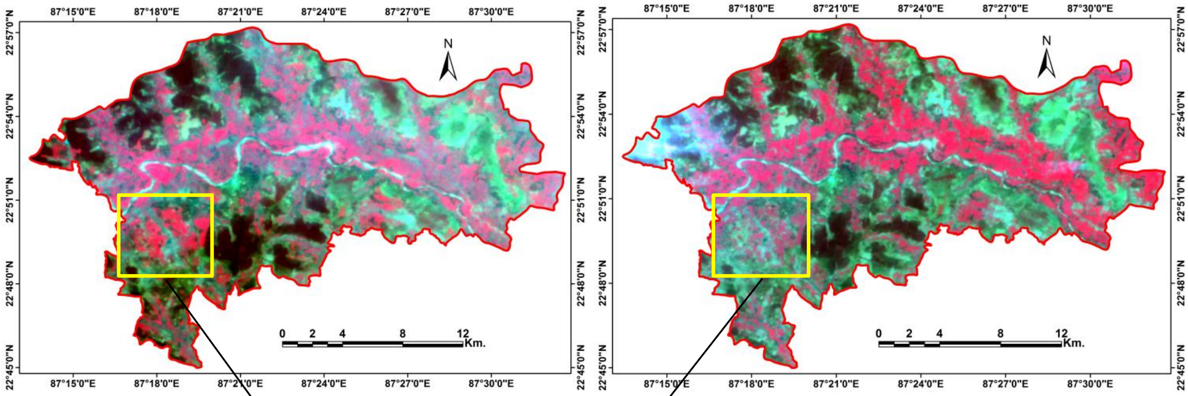

FCC of Garhbeta-1 Block on 25th January 2013 FCC of Garhbeta-1 Block on 04th February 2013

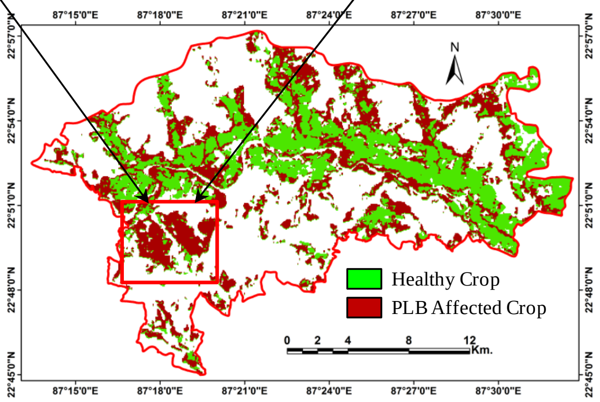

Classified Map of Healthy and Disease Affected Potato Crop of Garhbeta-1 Block

Figure 6.10: Visual Appearance of Healthy and Diseased Potato Crops of Garhbeta-1 Block

6.4.3.2 Rule Based Classification for Delineating PLB Affected Areas

Atmospherically corrected satellite data were classified by using rule based classification technique to segregate the disease affected potato crop pixels. This is being gone in two steps.

Step-1 : Enumeration of potato cultivated areas and classification of phonological phases (Described in Chapter 4)

Step-2 : Definitation of threshold : In the present study, NDVI threshold was used as criterion to discriminate between healthy and disease affected plants. The value of threshold was dynamic during the analysis process, which varied with crop growth phase.

Step-3 : Determination of area under PLB disease in different blocks of the study area form the classified map.

The classification map of potato late blight infestation is presented in figure 6.11.

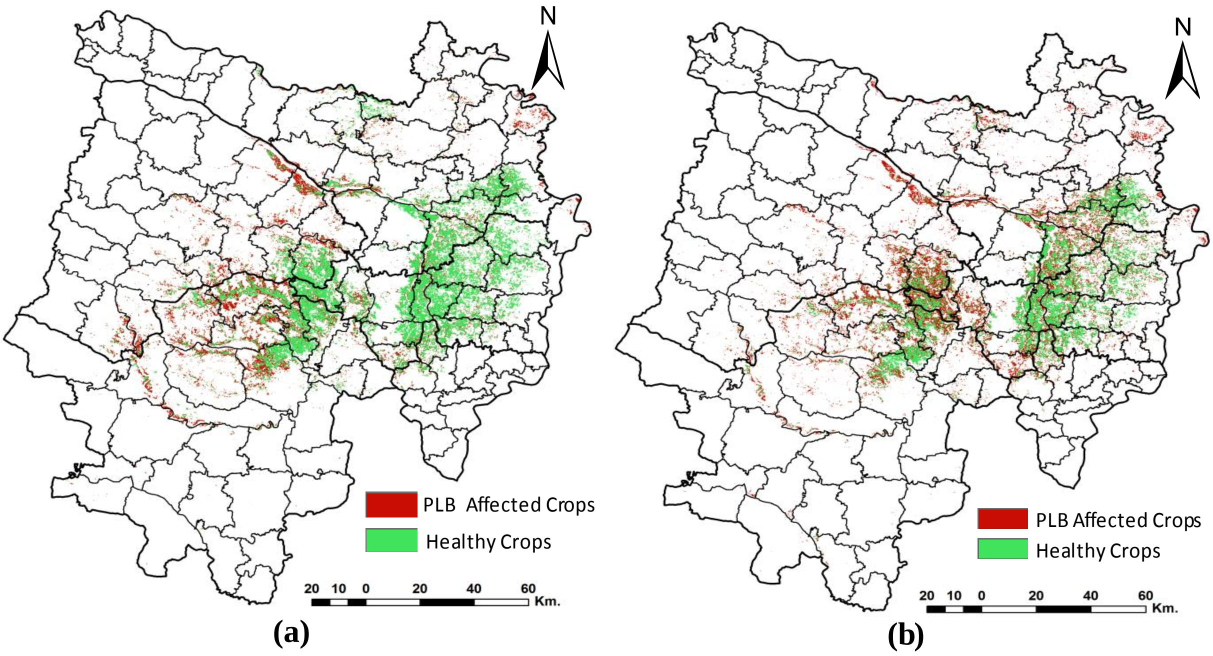

Figure 6.11: Block-wise Late Blight Affected Potato Crops Area in (a) 2012-13 (b) 2013-14

The Block-wise late blight affected potato areas were enumerated and presented in tabular form in Appendix B (B1) and Appendix B (B2) for the potato season of 2012-13 and 2013-14 respectively.

In 2012-13 blight affected potato area was found to be maximum in Paschim Medinipur district where more than 50% potato cultivated areas have been affected by potato blight in seven blocks. Those include, Jhargram (74.1%), Kharagpur I (58.4%), Medinipur (56.7%), Kharagpur II (52.5%), Binpur I (55.2%), Salbani (52.9%) and Garhbeta III (50.8%). In Burdwan PLB damage in more than 50% of potato grown areas was recorded in 5 blocks that include, Purbasthali II (62.4%), Katwa I (61%), Galsi I (60.1%), Katwa II (56.5%) and Ketugram I (52.6%). In Bankura district five blocks were found to be affected by PLB in more than 50% of potato grown areas. Those blocks include, Patrasayer (69.6%), Sonamukhi (57.6%), Indus (52.8%), Raipur (51.9%) and Taldangra (51.8%). The potato blight infestation was very less in Hoogly and Howrah districts.

In 2013-14, the disease scenario was different from that of previous year. Three blocks of Paschim Medinipur district were severely affected by potato late blight (more than 50% potato grown areas). They include, Binpur II (66.9%), Gopiballavpur II (65.9%) and Garbeta I (52.9%). In Hoogly three blocks were affected. They include Goghat II (64.3%), Arambag (64.1%) and Goghat I (58.7%). In Bankura three blocks where more than 50% potato grown areas were infested by potato late blight are Kotulpur (68.5%), Sonamukhi (57%) andPatrasayer (50.1%). In Burdwan maximum PLB infestation was recorded from Ketugram I block where 93% potato grown areas have been infested. Other blocks infested by potato blight include, Kanksa (55.25%) and Khandaghosh (55%).

6.4.3.3 Validation of the Results

Satellite based estimation of PLB area was compared with PLB reported areas of Department of Agriculture, Government of West Bengal. The summary statistics is shown in Table 6.8. In 2012-13 potato growing season, the value of RMSE between estimated area and reported area of PLB infestation was 6.38 and the coefficient of determination (R^2) of 0.88. In 2013-14 potato growing season the RMSE value was little higher (10.47) with the coefficient of determination (R^2) value of 0.85.

Generally, the lower RMSE value represents the better predictive capability of a model in terms of its absolute deviation and similarly, higher coefficient of determination indicated higher accuracy of the estimated value. However, in the first year of study, the total areas and number of cases of PLB infestation was more and that influenced the RMSE and coefficient of determination. The relative root mean square error (rRMSE) showed lower value (0.07) in the second year (2013-14) as compared to the first year (0.10) which indicate better model accuracy in 2013-14.

The Coefficient of Resudial Mass (CRM) indicates the overall under- or over-estimations in case of the +ve values and –ve values respectively. The value would be zero for perfect estimation. The CRM value was 0.17 for the cropping year of 2012-13 and 0.09 for the cropping year of 2013-14 respectively which indicates the slight underestimation of overall measurement values. The D-index was very high with 0.94 and 0.95 in 2012-13 and 2013-14 respectively. D-index intended to be a descriptive measure to make cross-comparisons in between estimated and measured values. In both consecutive cropping years Modelling Efficiency (ME) showed the values of 0.74 and 0.78 which indicating relatively good performance. The overall results of these comparisons well matched with the measured values.

Table-6.8: Statistical Performance Indicators

Cropping Year	RMSE	rRMSE	CRM	D-Index	ME	R^2
2012-13	6.38	0.10	0.17	0.94	0.74	0.88*
2013-14	10.47	0.07	0.09	0.95	0.78	0.85*

** all values are significant at 95% confidence level*

6.4.4 PLB Disease Intensity or Severity Model

The regression analysis of showed significant correlation of different spectral vegetation indices with the disease intensity as discussed in earlier sections. Based on those analysis two independent predictor variables viz. NDVI and PCCF having significant relation with potato late blight disease severity were selected and linear multiple regression equation was developed using the data of both the years (2012-13 and 2013-14). Linear regression model was used to estimate the late blight disease severity using selected spectral indices (NDVI and PCCF). The multiple regression model is given below.

$$DSI=12.70 – (9.71*NDVI) – (0.08*PCCF) \quad (r^2 = 0.865) \ldots\ldots (14)$$

A total of 54 independent samples, having different intensity of PLB disease, over the years, were used for model validation which were kept separate and not used for model development. Mean RMSE was calculated using modelled and measured values of Disease Severity Index. The value of RMSE in between measured and predicted disease intensity is least i.e. 1.22 when considering NDVI and PCCF which is considered to be fairly well.

The multi regression model was used to generate disease severity maps and those were classified as per the disease severity indices using appropriate threshold (0 – 8 DSI values). Results are presented in Figure 6.12 to 6.21.

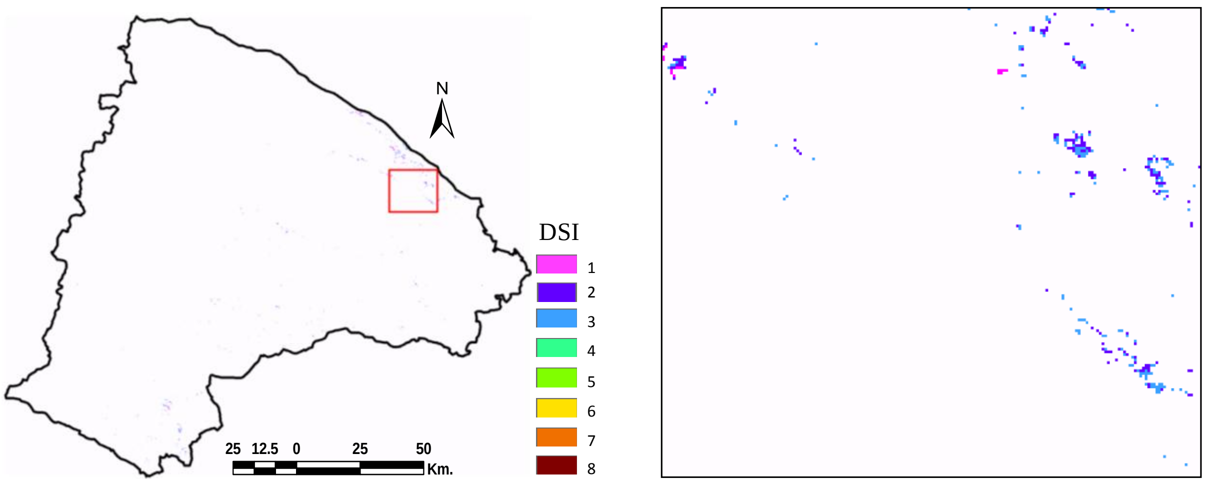
N
DSI
1
2
3
4
5
6
7
8
25 12.5 0 25 50
Km.

(a)

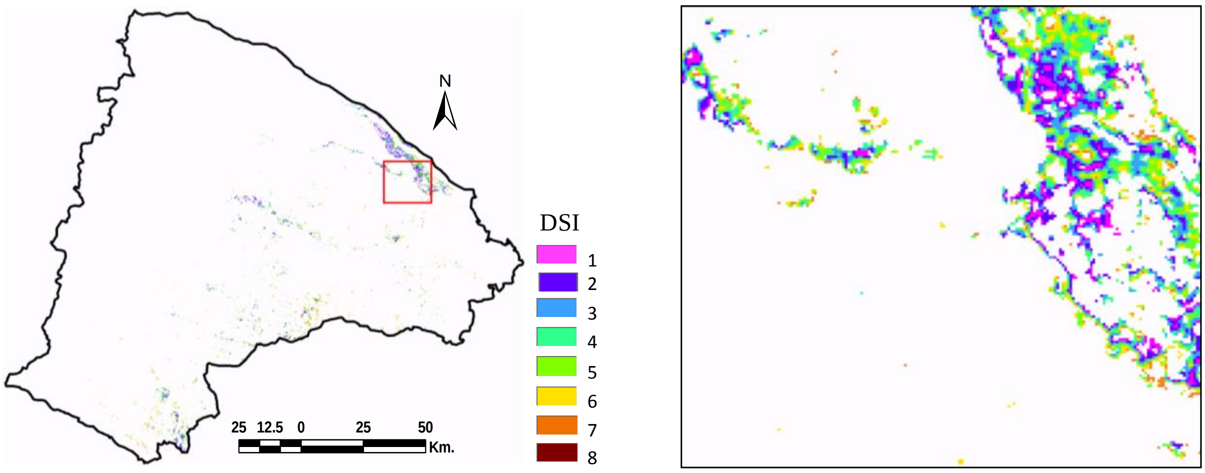
N
DSI
1
2
3
4
5
6
7
8
25 12.5 0 25 50
Km.

(b)

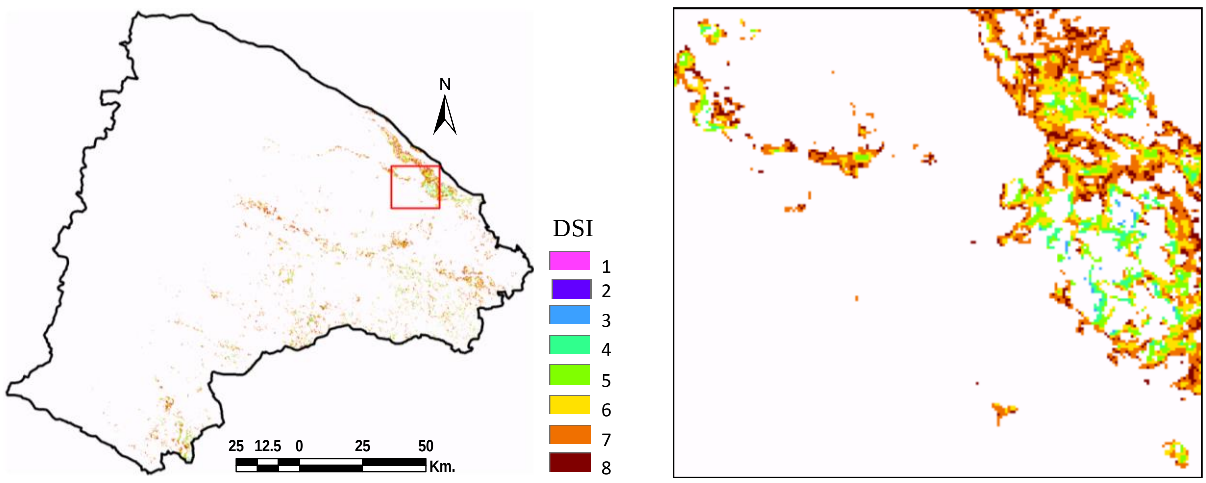
N
DSI
1
2
3
4
5
6
7
8
25 12.5 0 25 50
Km.

(c)

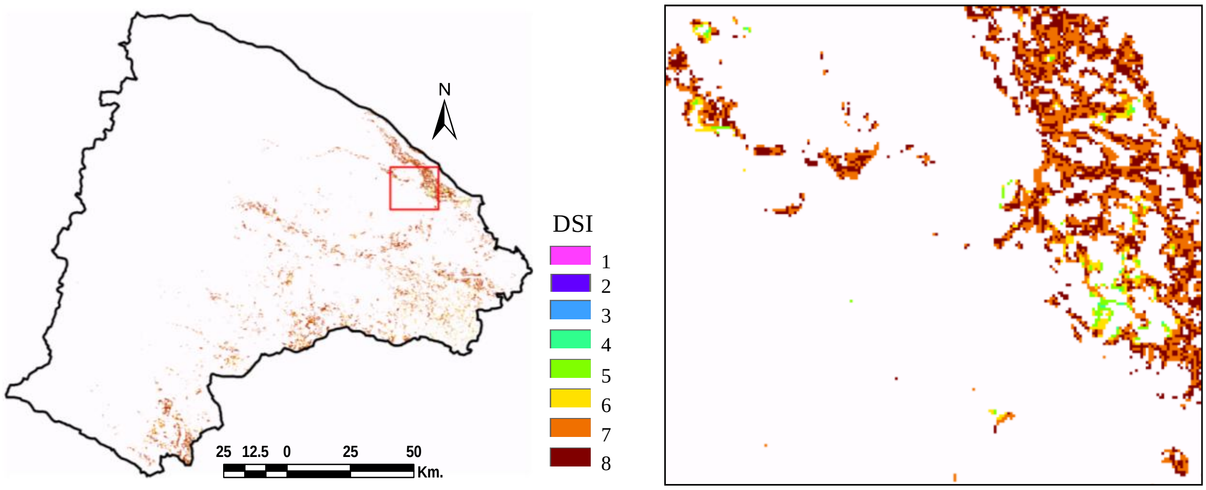

(d)

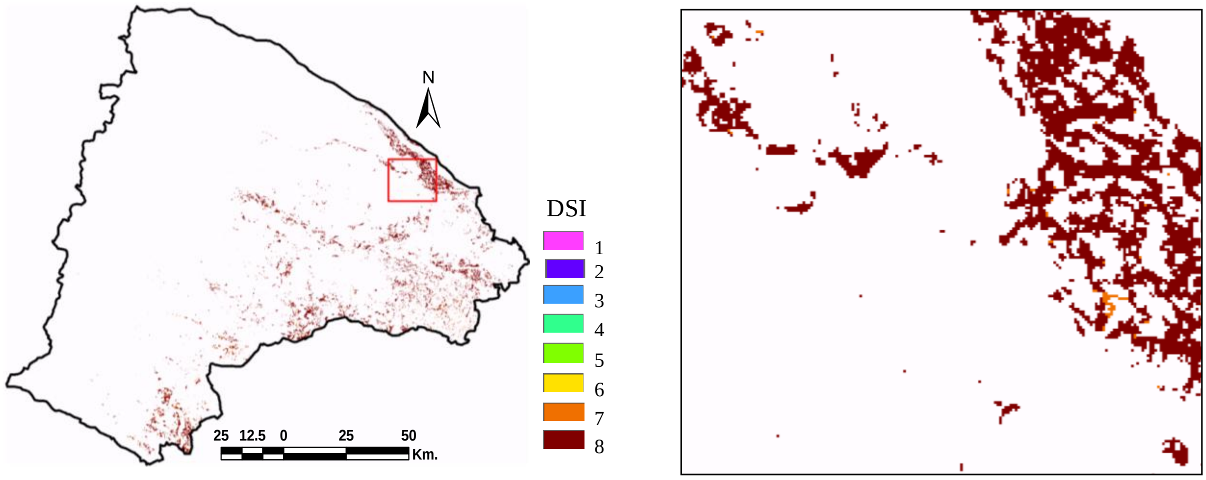

(e)

Figure 6.12: Potato Late Blight Disease Severity Over the Observation Dates in Bankura District with Zoomed View on (a) 15th Jan 13 (b) 25th Jan 13 (c) 04th Feb 13 (d) 23rd Feb 13 (e) 28th Feb 13

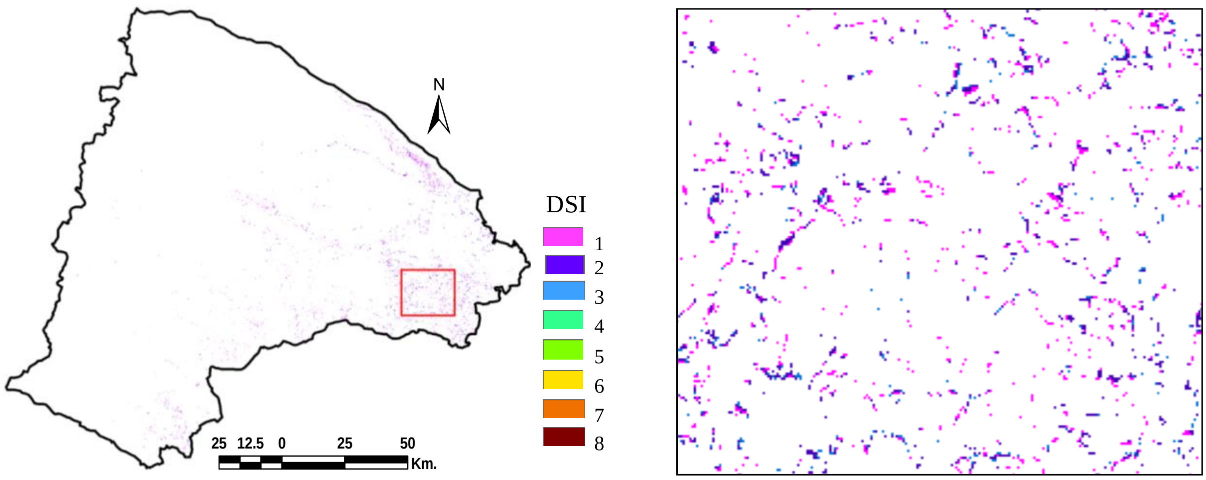

(a)

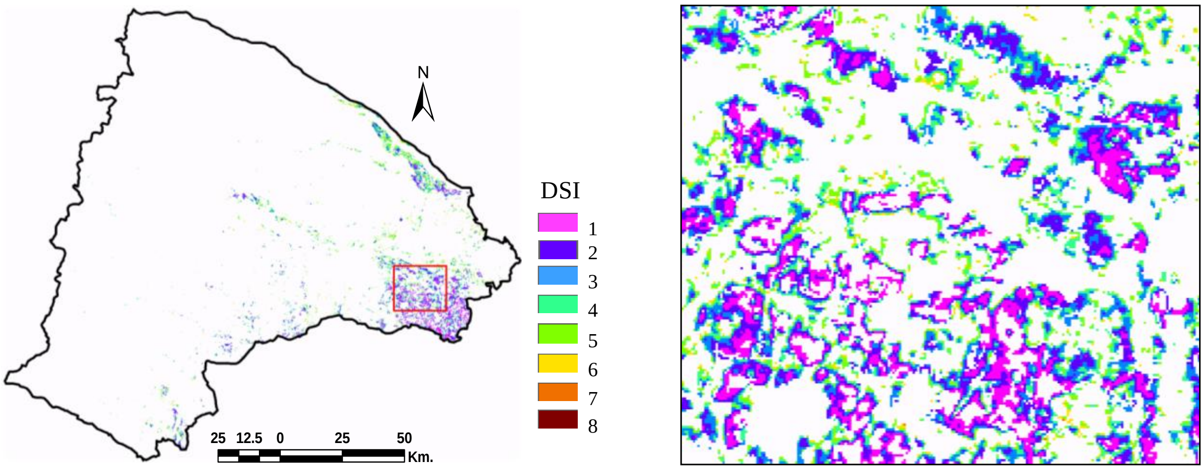

(b)

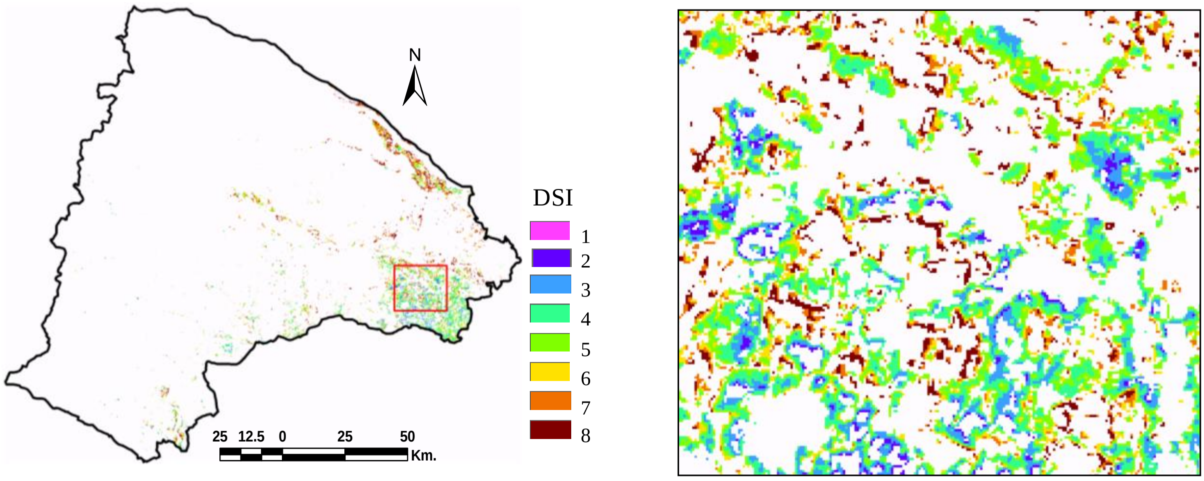

(c)

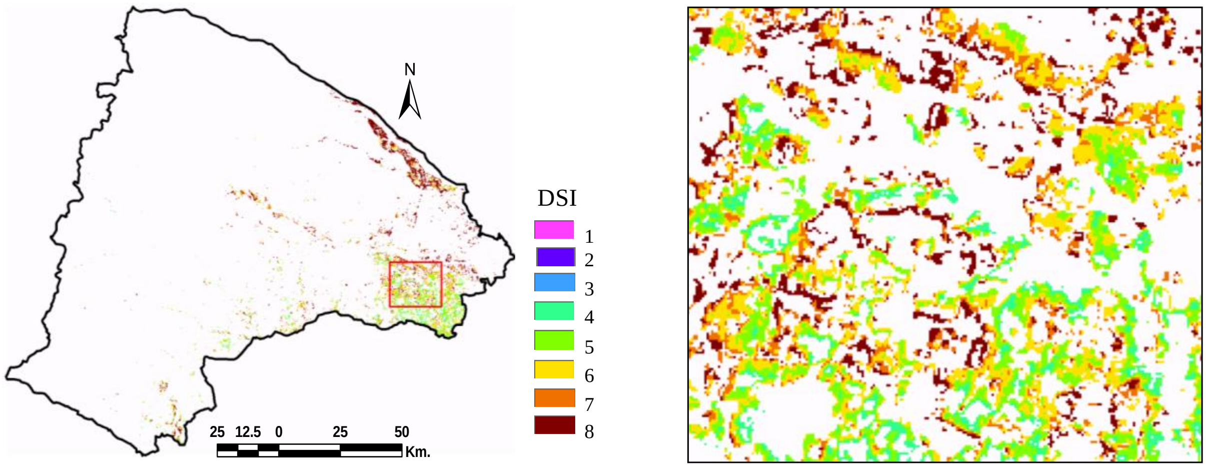

(d)

Figure 6.13: Potato Late Blight Disease Severity Over the Observation Dates in Bankura District with Zoomed View on (a) 10th Jan 14 (b) 25th Jan 14 (c) 13th Feb 14 (d) 18th Feb 14

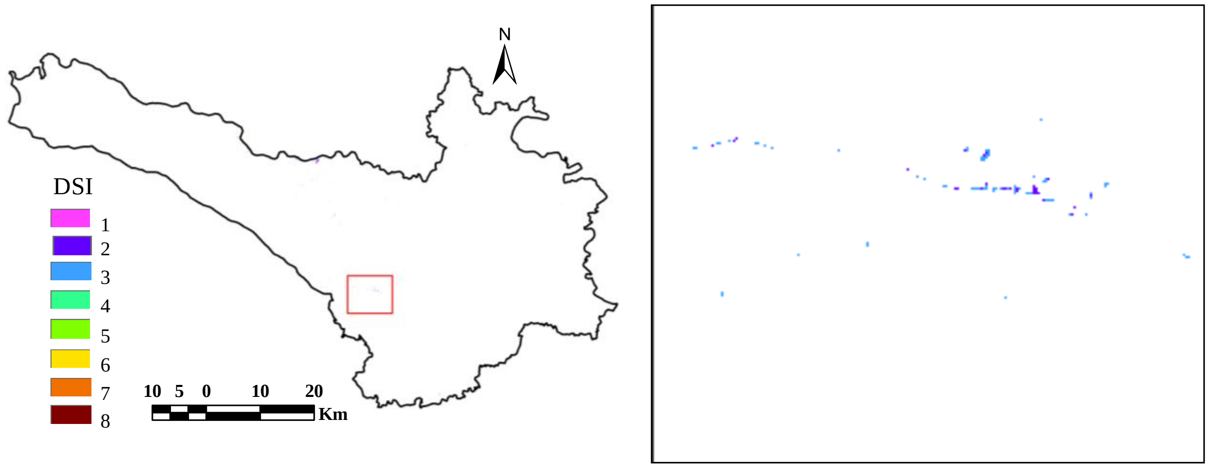
N
DSI
1
2
3
4
5
6
7
8
10 5 0 10 20
Km

(a)

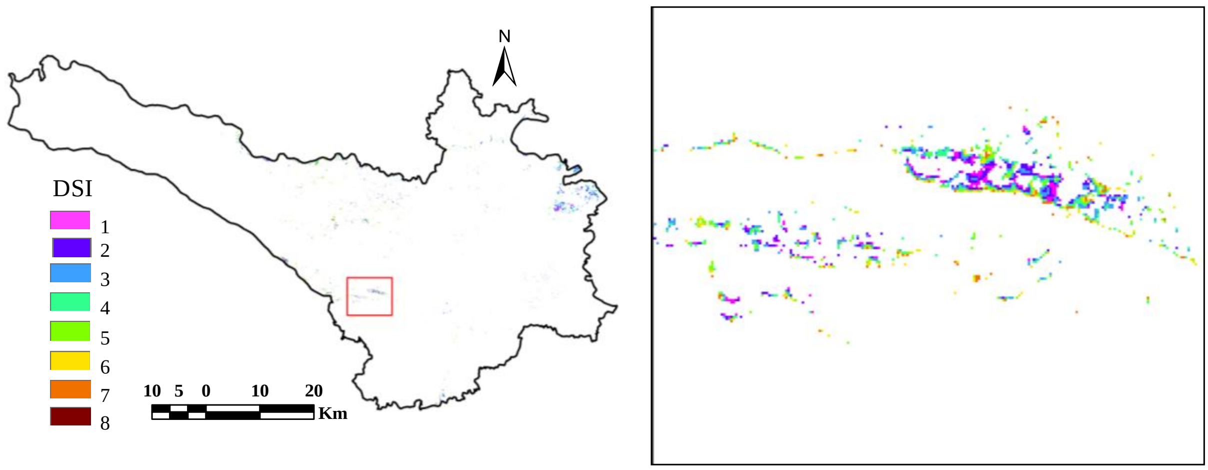
N
DSI
1
2
3
4
5
6
7
8
10 5 0 10 20
Km

(b)

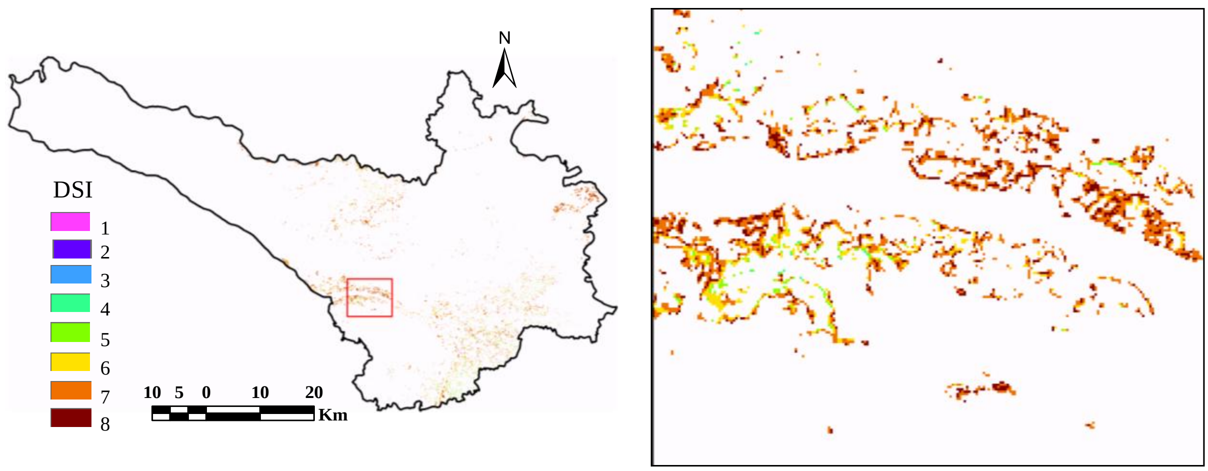
N
DSI
1
2
3
4
5
6
7
8
10 5 0 10 20
Km

(c)

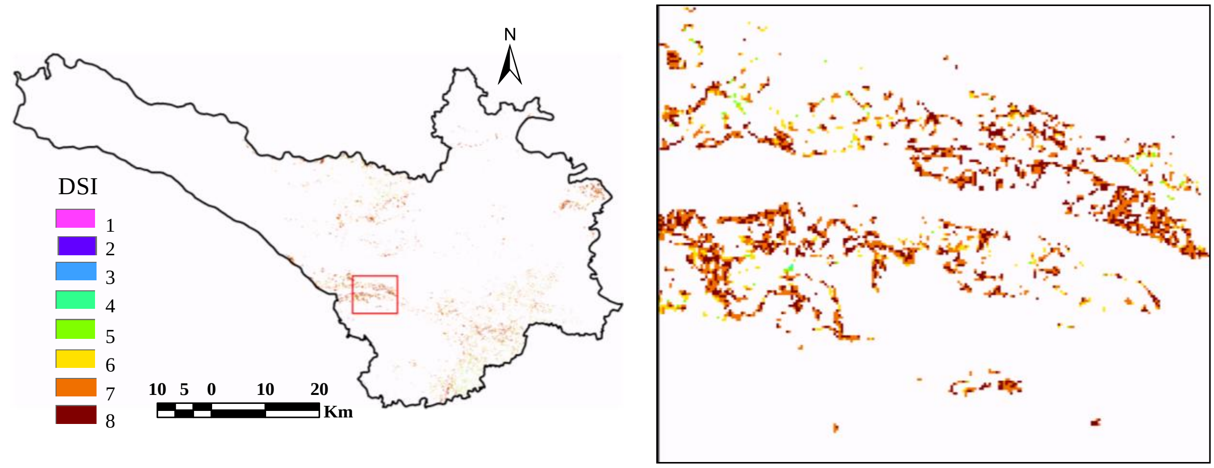

(d)

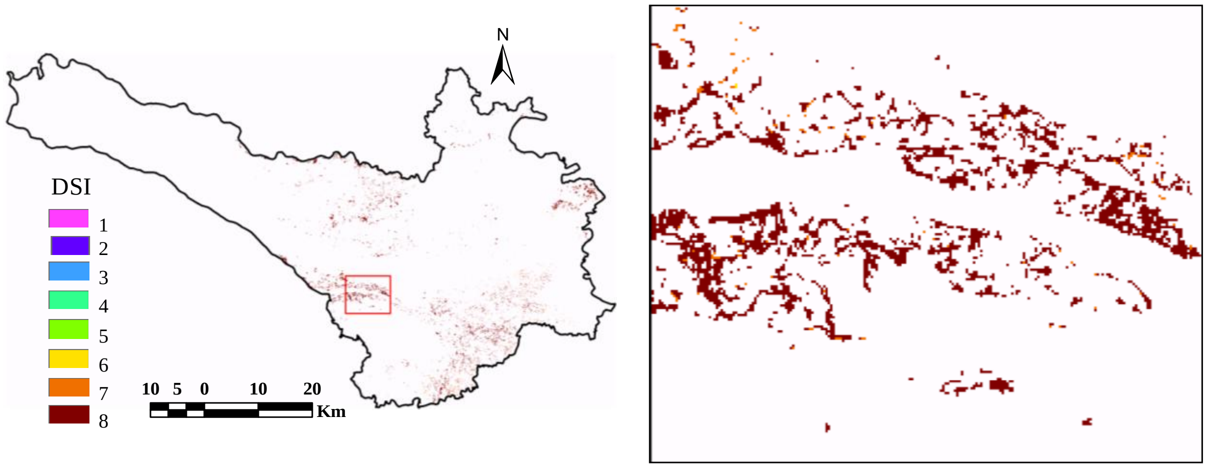

(e)

Figure 6.14: Potato Late Blight Disease Severity Over the Observation Dates in Burdwan District with Zoomed View on (a) 15th Jan 13 (b) 25th Jan 13 (c) 04th Feb 13 (d) 23rd Feb 13 (e) 28th Feb 13

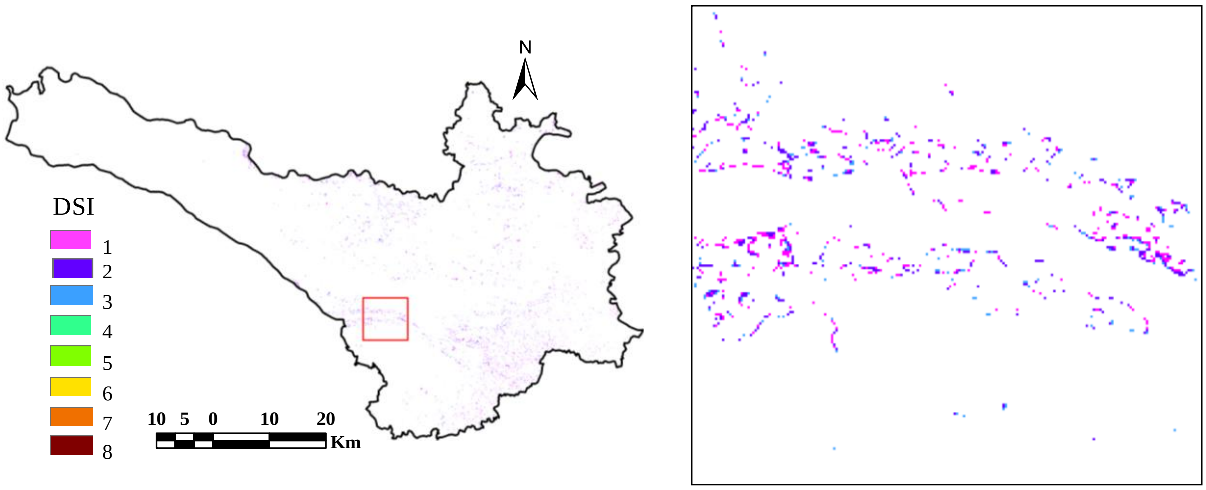

(a)

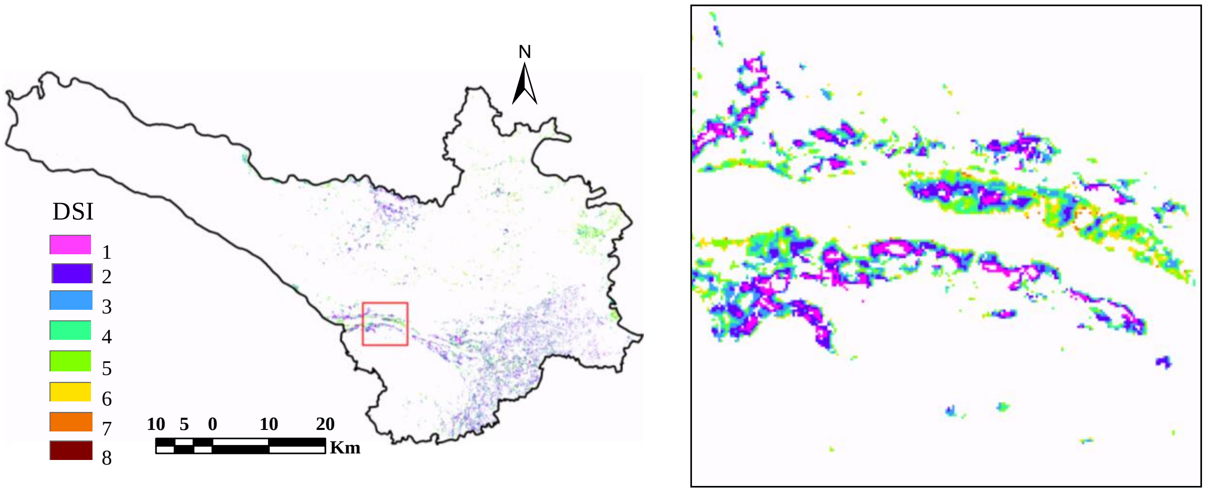

(b)

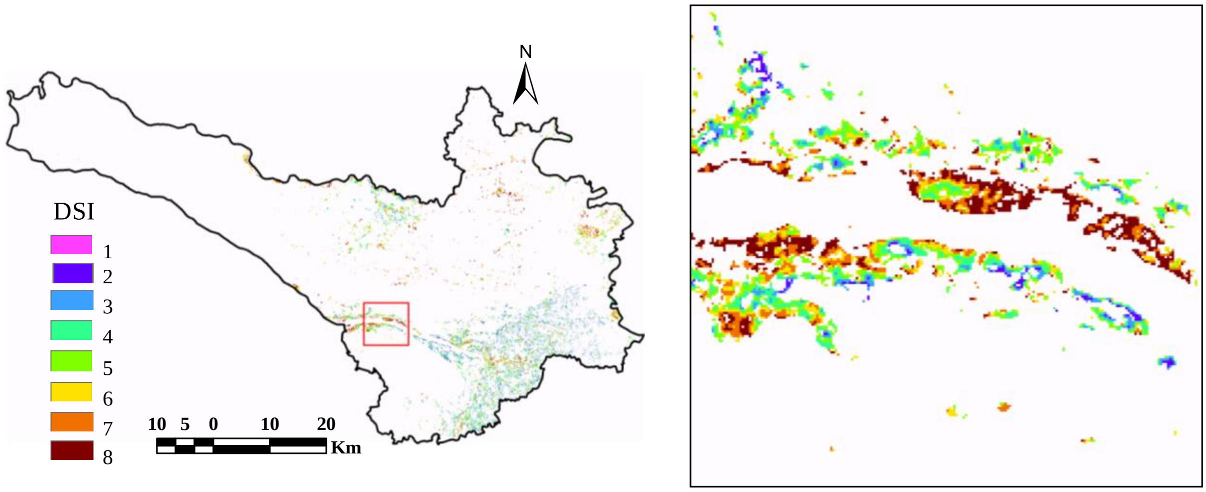

(c)

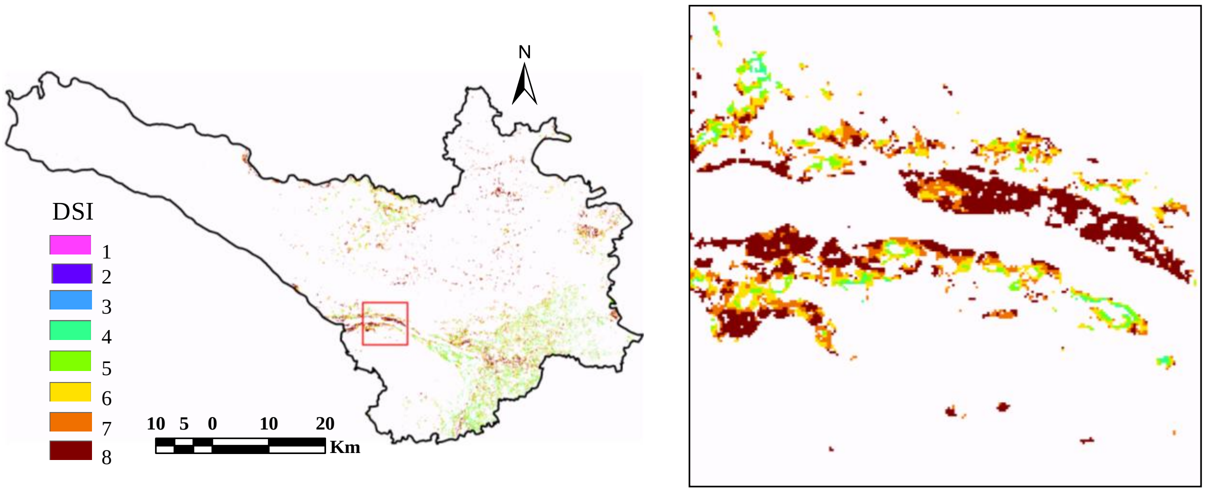

(d)

Figure 6.15: Potato Late Blight Disease Severity Over the Observation Dates in Burdwan District with Zoomed View on (a) 10th Jan 14 (b) 25th Jan 14 (c) 13th Feb 14 (d) 18th Feb 14

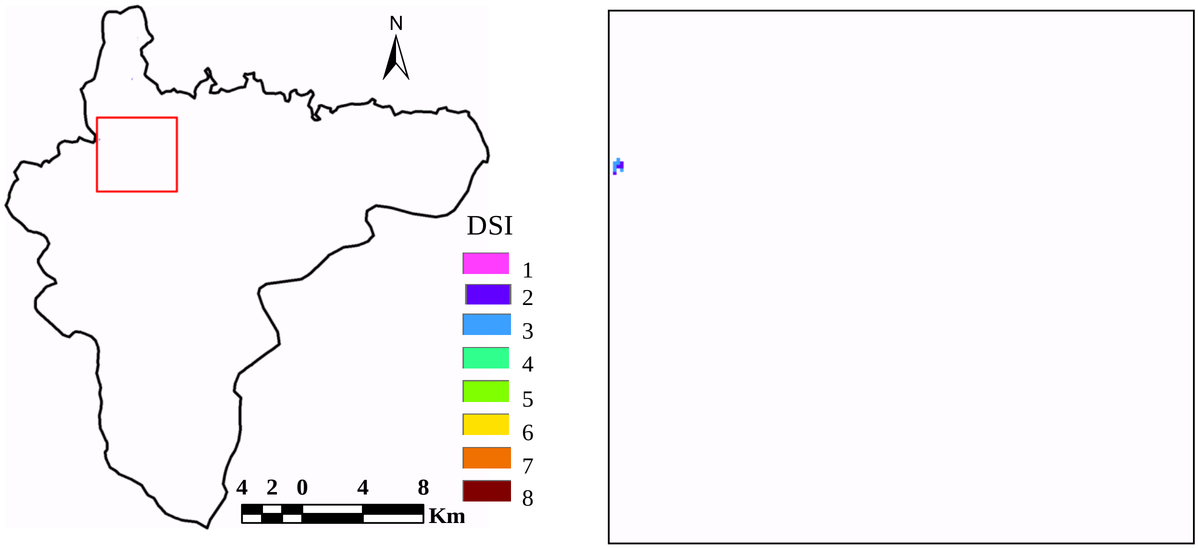
N
DSI
1
2
3
4
5
6
7
8
4 2 0 4 8
Km

(a)

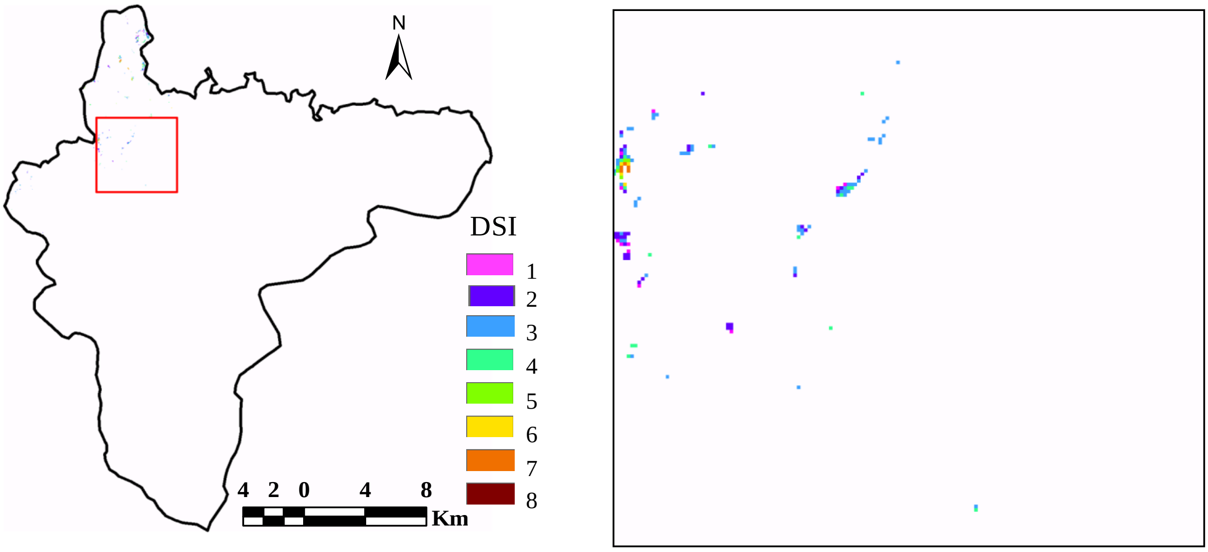
N
DSI
1
2
3
4
5
6
7
8
4 2 0 4 8
Km

(b)

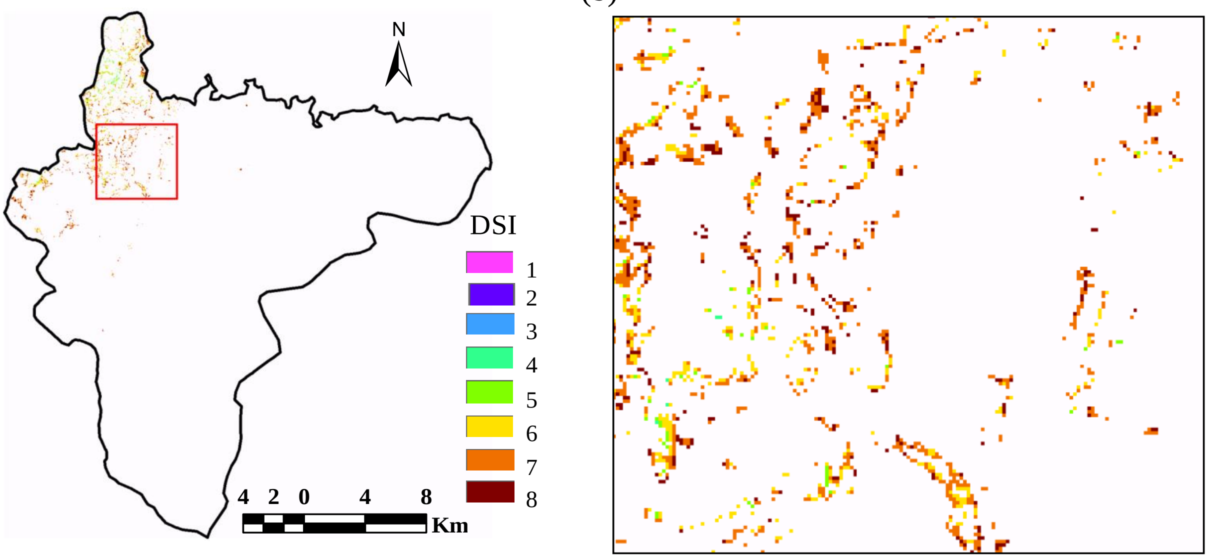
N
DSI
1
2
3
4
5
6
7
8
4 2 0 4 8
Km

(c)

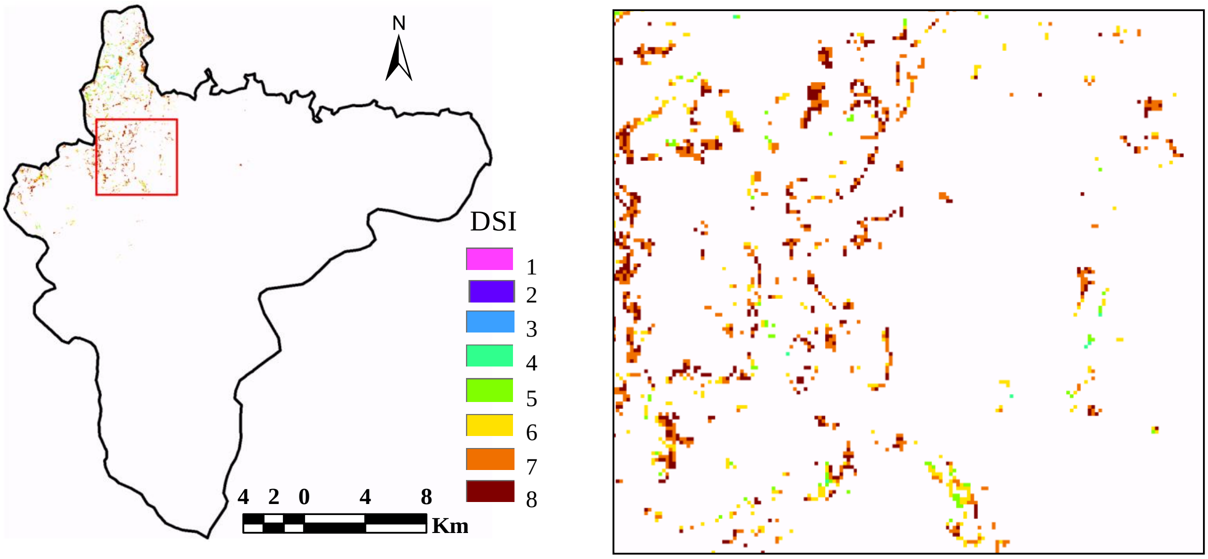

(d)

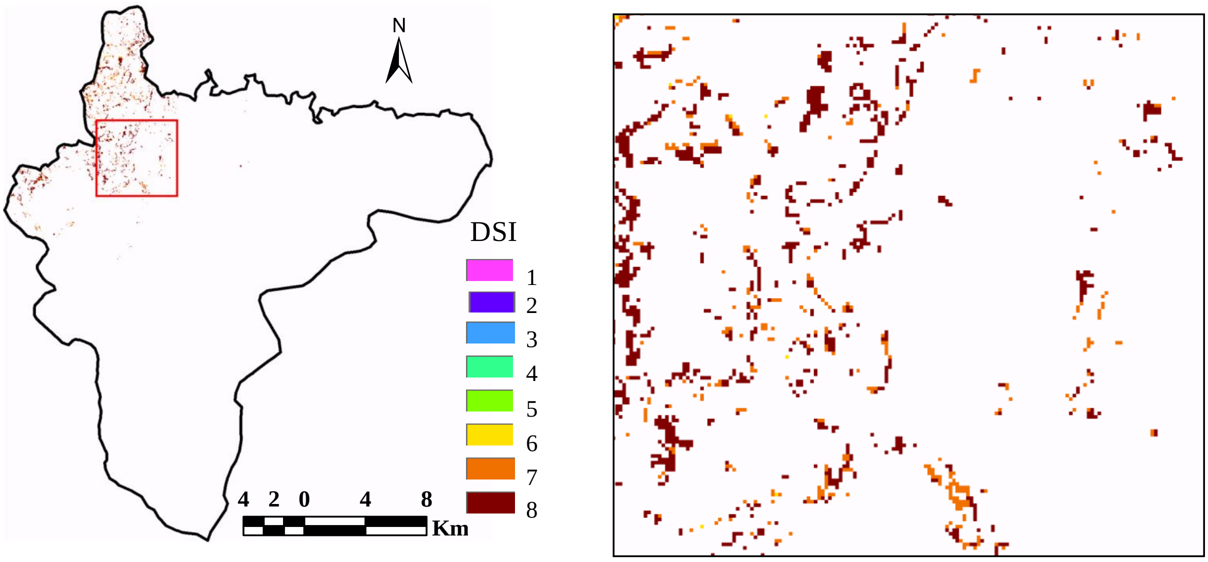

(e)

Figure 6.16: Potato Late Blight Disease Severity Over the Observation Dates in Howrah District with Zoomed View on (a) 15th Jan 13 (b) 25th Jan 13 (c) 04th Feb 13 (d) 23rd Feb 13 (e) 28th Feb 13

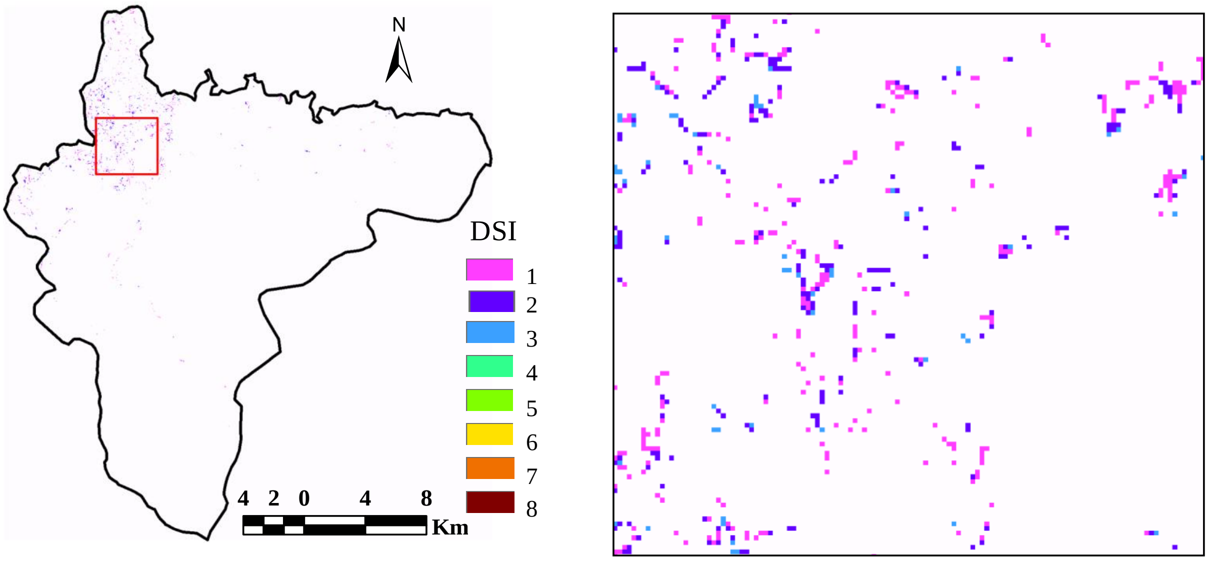
N
DSI
1
2
3
4
5
6
7
8
4 2 0 4 8
Km

(a)

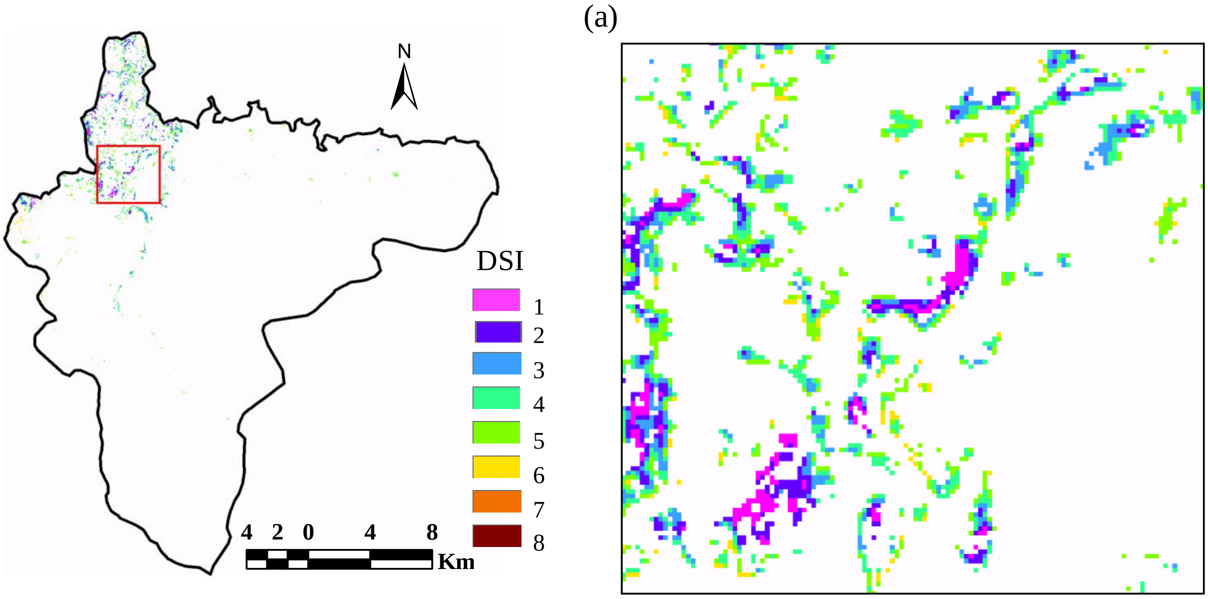
N
DSI
1
2
3
4
5
6
7
8
4 2 0 4 8
Km

(b)

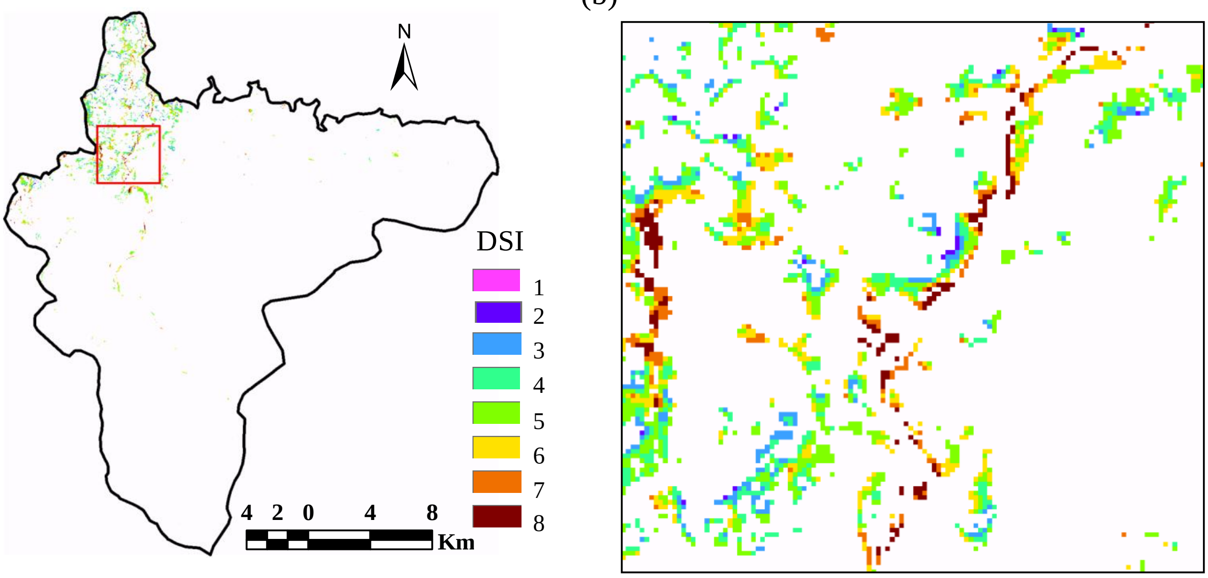
N
DSI
1
2
3
4
5
6
7
8
4 2 0 4 8
Km

(c)

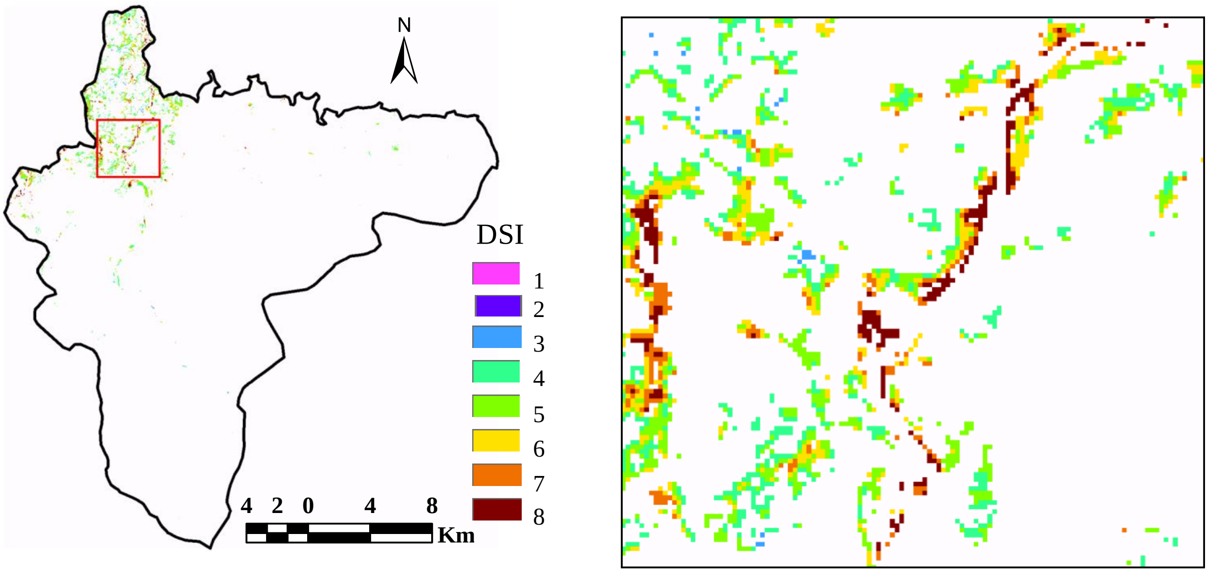

(d)

Figure 6.17: Potato Late Blight Disease Severity Over the Observation Dates in Howrah District with Zoomed View on (a) 10th Jan 14 (b) 25th Jan 14 (c) 13th Feb 14 (d) 18th Feb 14

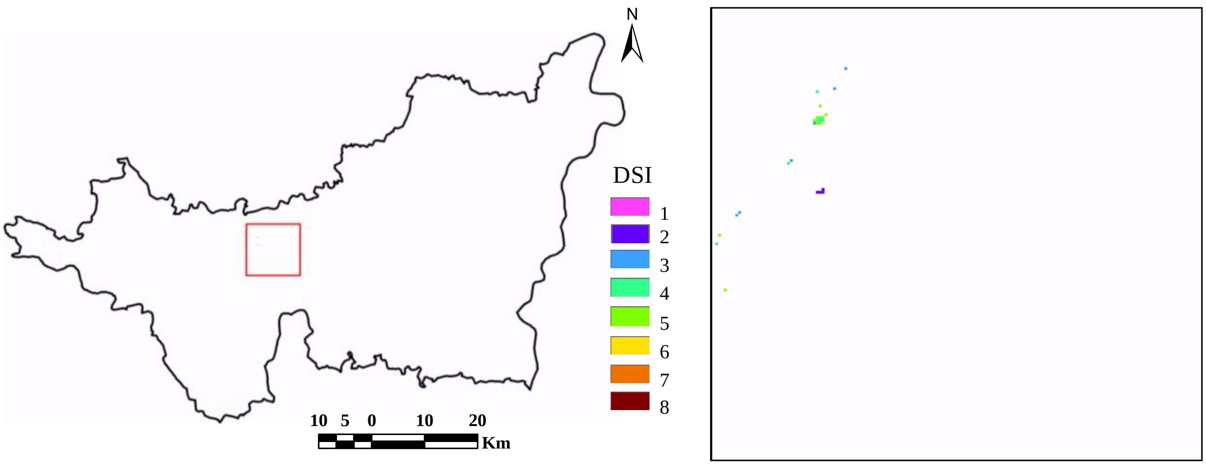

(a)

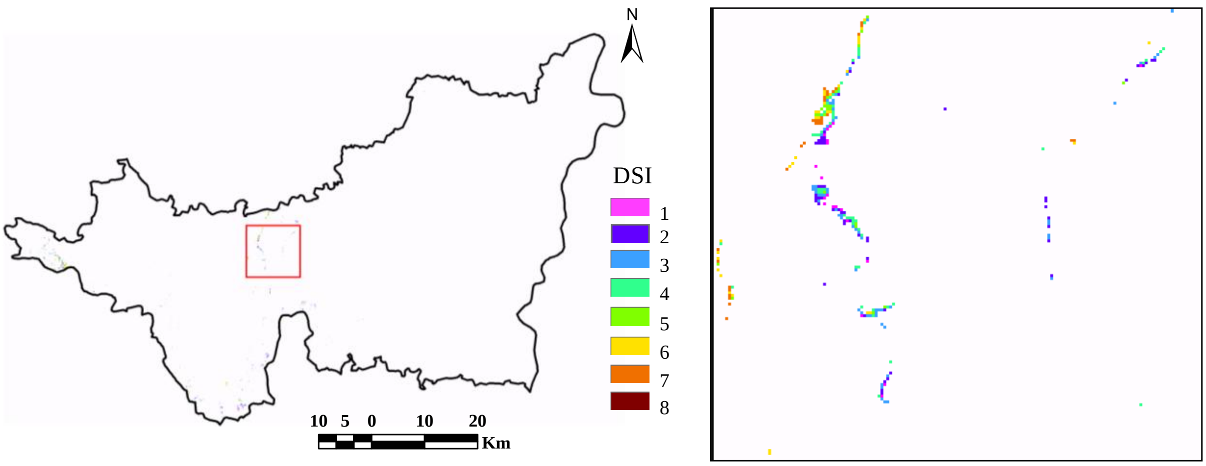

(b)

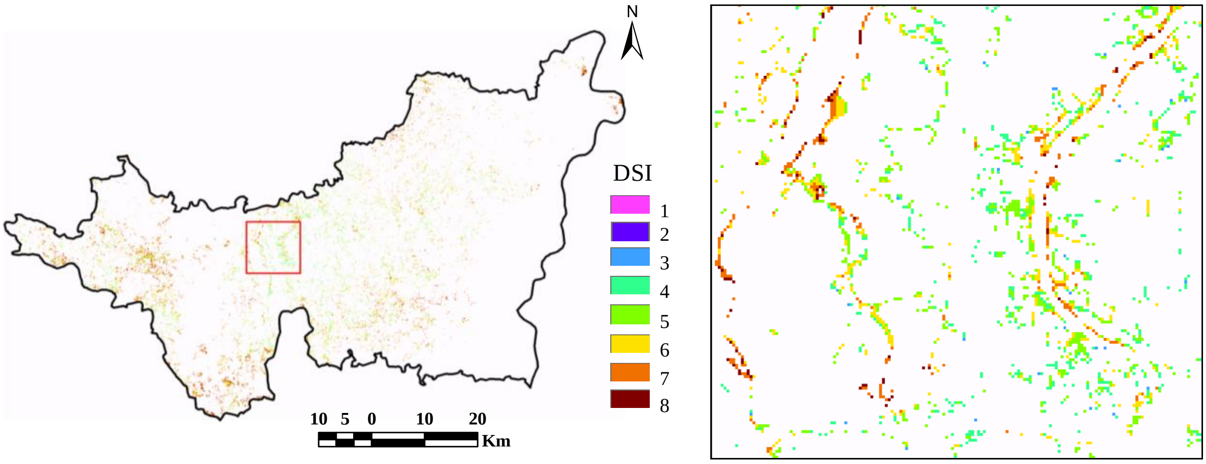

(c)

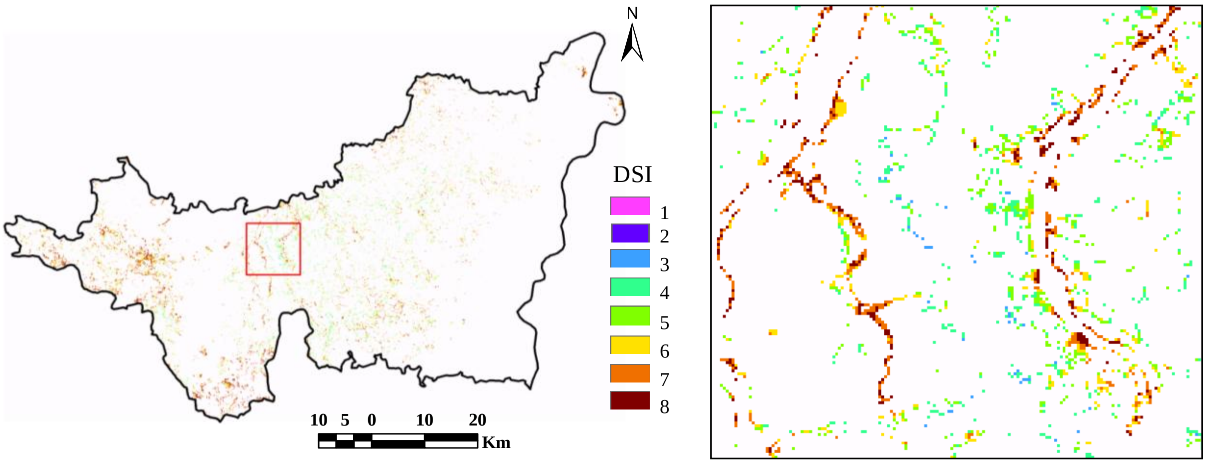

(d)

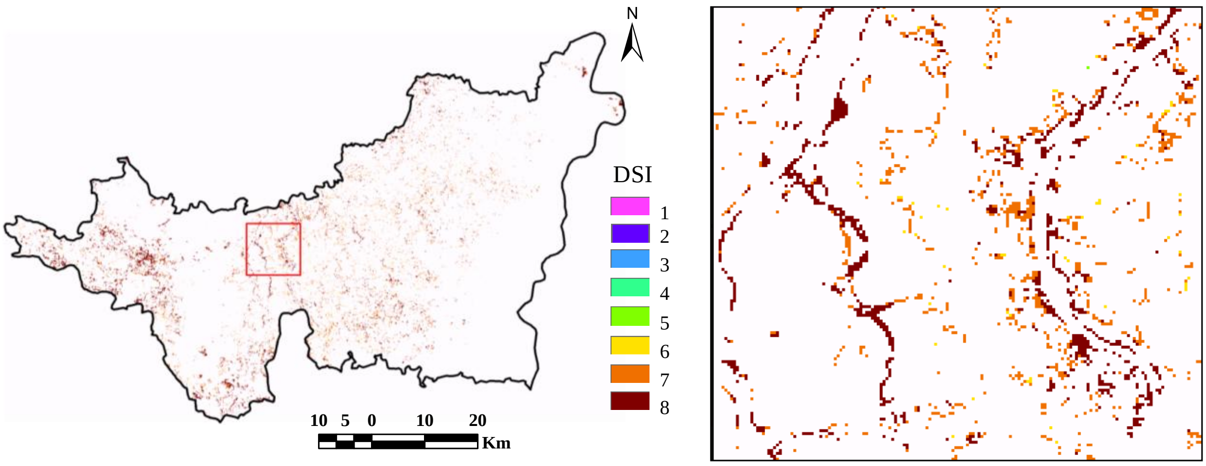

(e)

Figure 6.18: Potato Late Blight Disease Severity Over the Observation Dates in Hooghly District with Zoomed View on (a) 15th Jan 13 (b) 25th Jan 13 (c) 04th Feb 13 (d) 23rd Feb 13 (e) 28th Feb 13

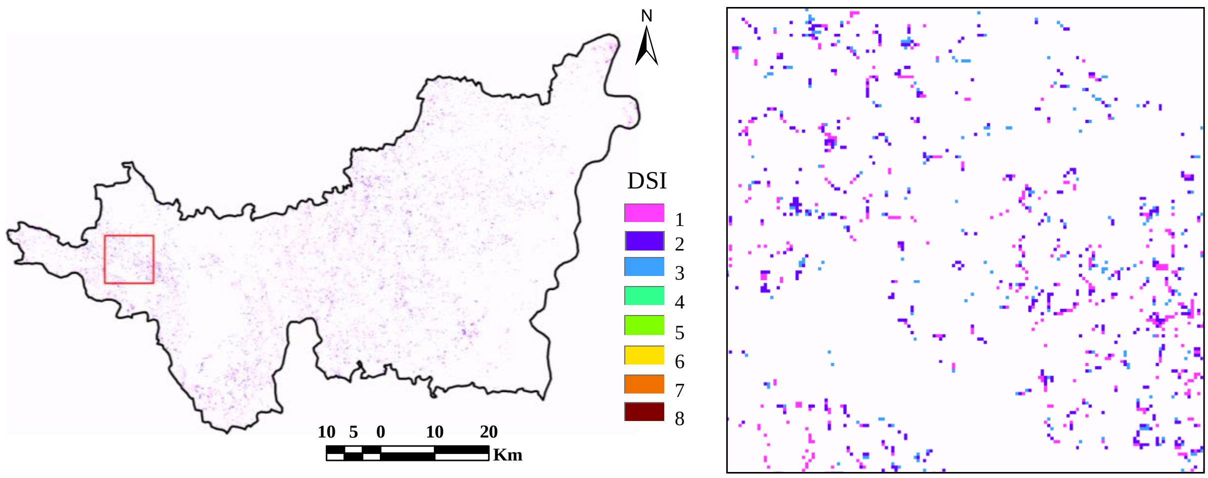
N
DSI
1
2
3
4
5
6
7
8
10 5 0 10 20
Km

(a)

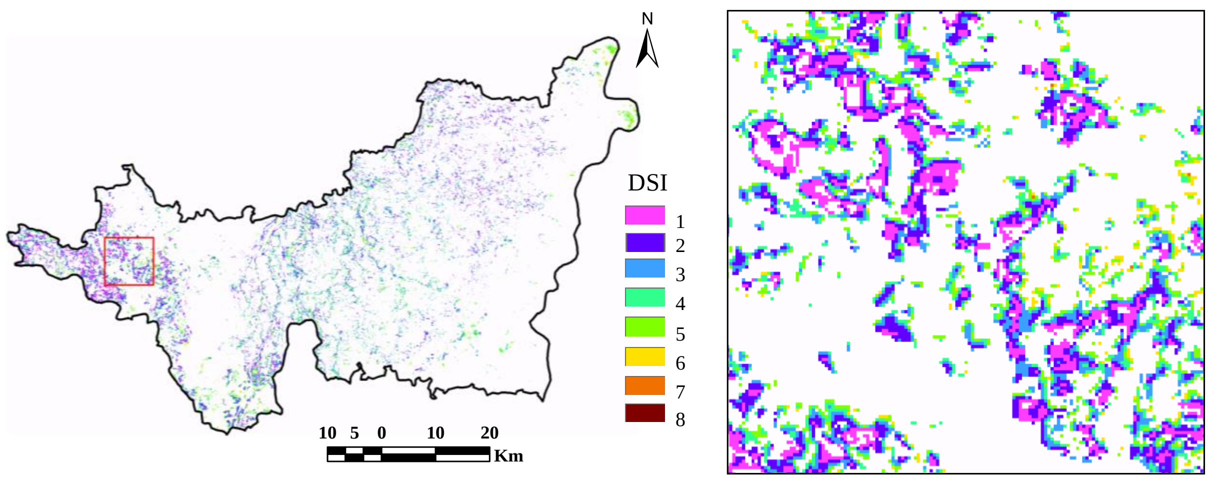
N
DSI
1
2
3
4
5
6
7
8
10 5 0 10 20
Km

(b)

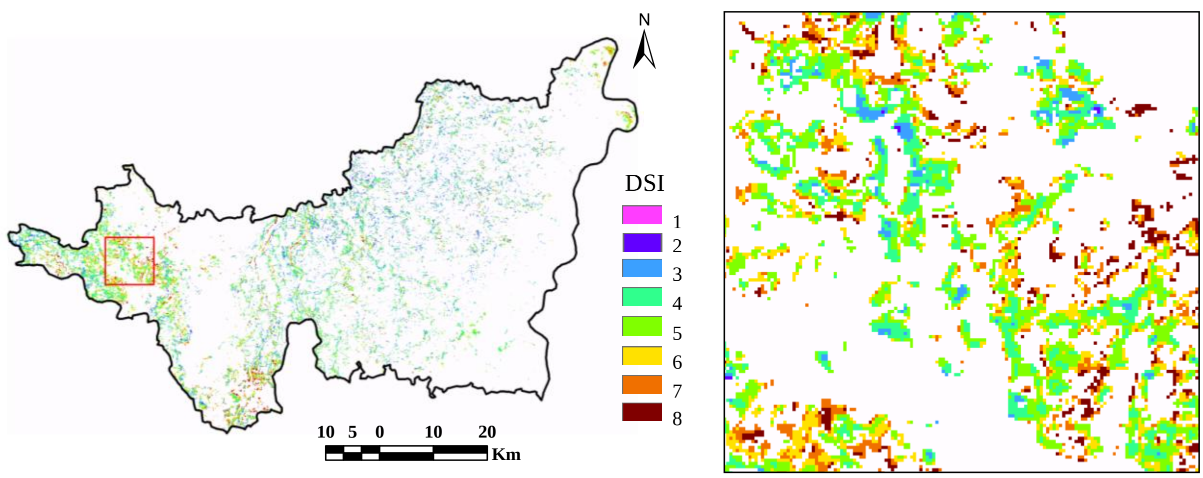
N
DSI
1
2
3
4
5
6
7
8
10 5 0 10 20
Km

(c)

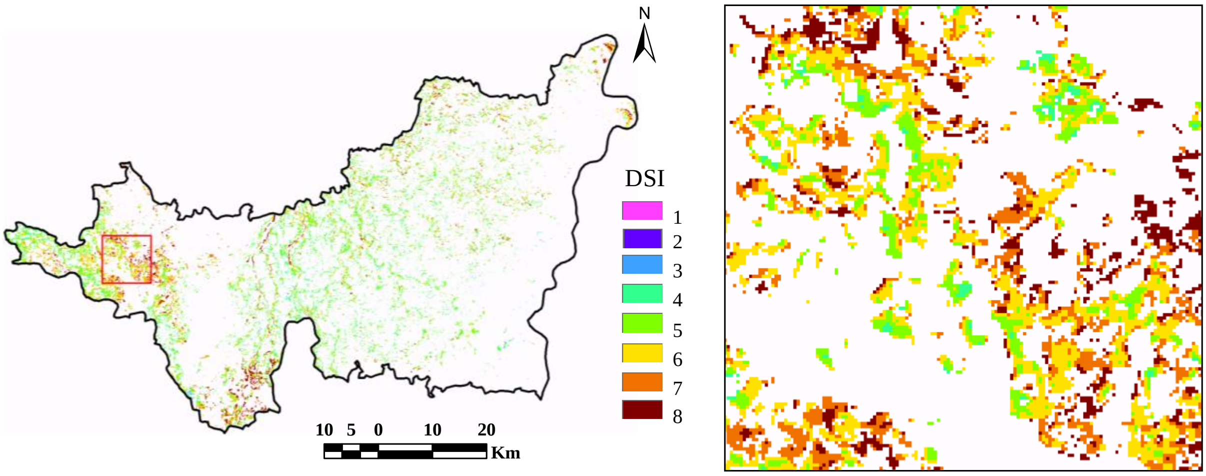

(d)

Figure 6.19: Potato Late Blight Disease Severity Over the Observation Dates in Hooghly District with Zoomed View on (a) 10th Jan 14 (b) 25th Jan 14 (c) 13th Feb 14 (d) 18th Feb 14

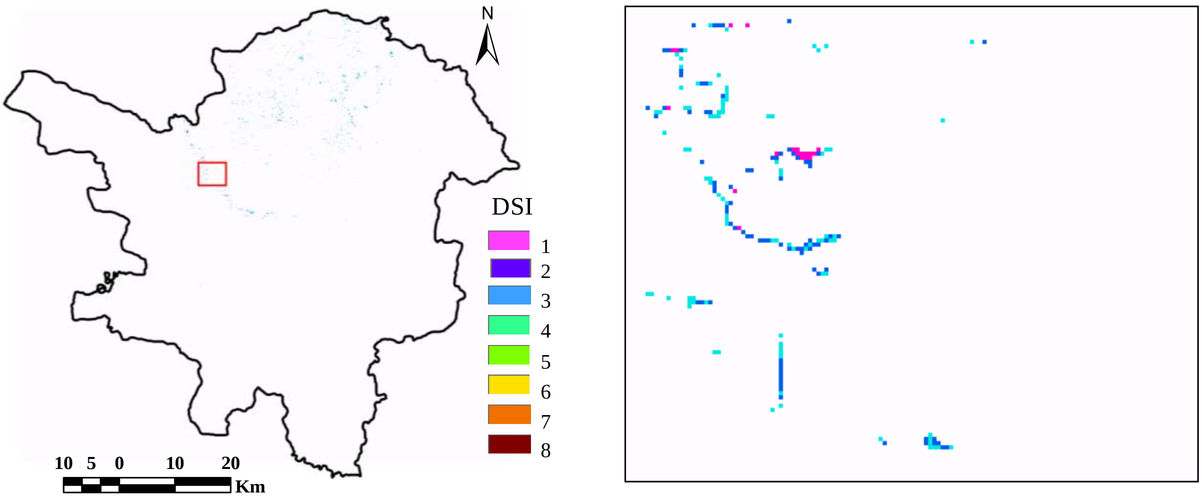

(a)

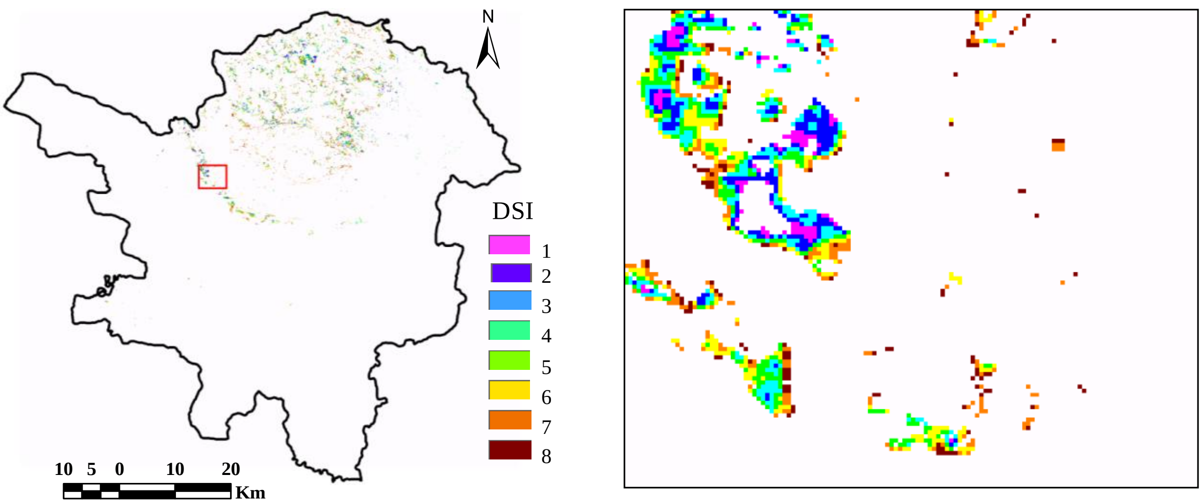

(b)

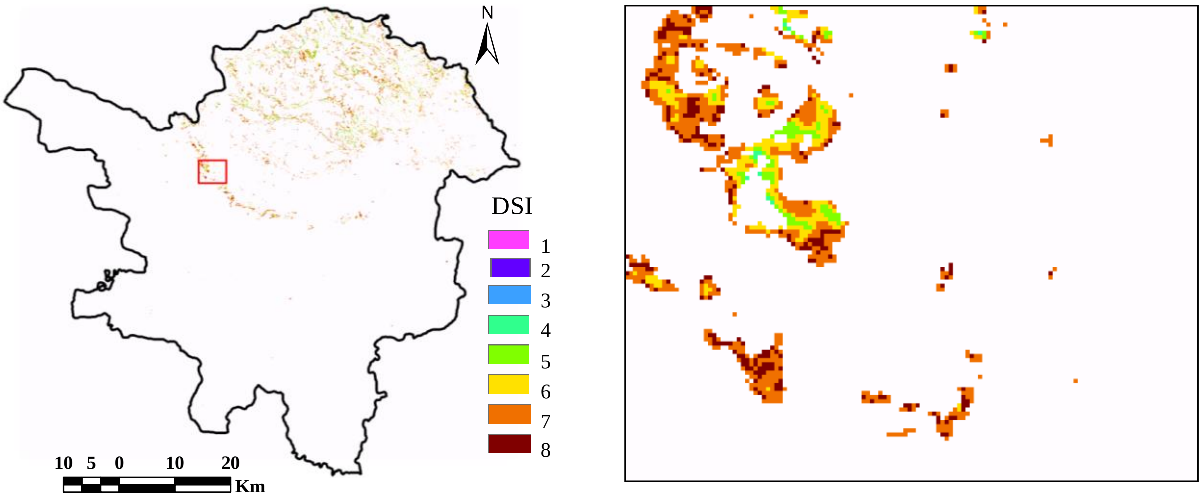

(c)

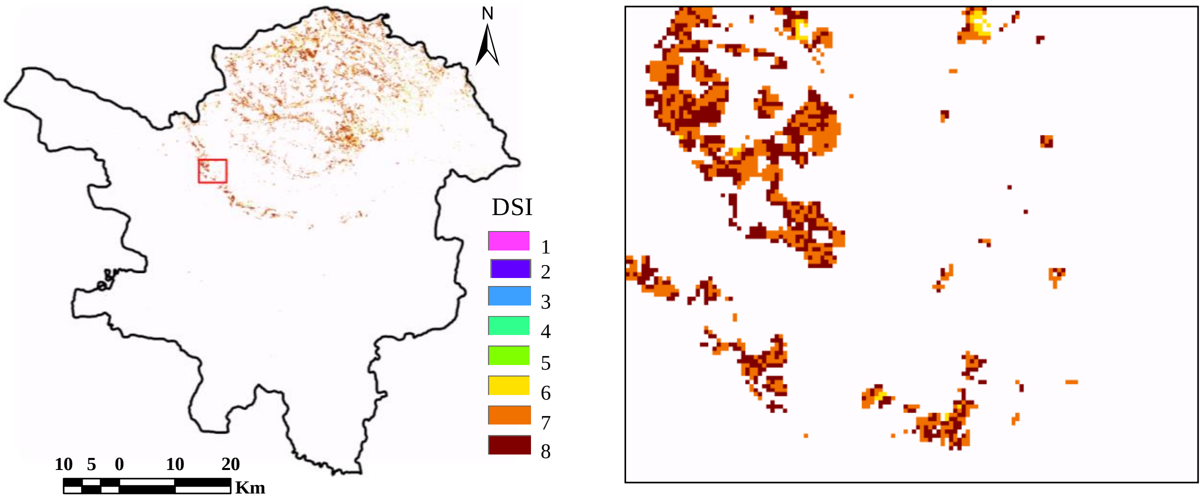

(d)

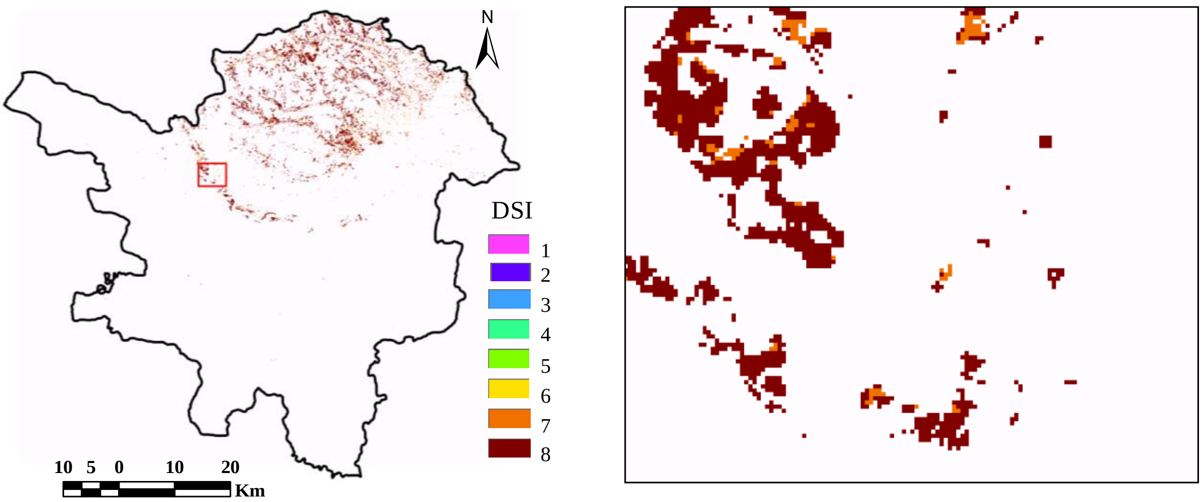

(e)

Figure 6.20: Potato Late Blight Disease Severity Over the Observation Dates in Paschim Medinipur District with Zoomed View on (a) 15th Jan 13 (b) 25th Jan 13 (c) 04th Feb 13 (d) 23rd Feb 13 (e) 28th Feb 13

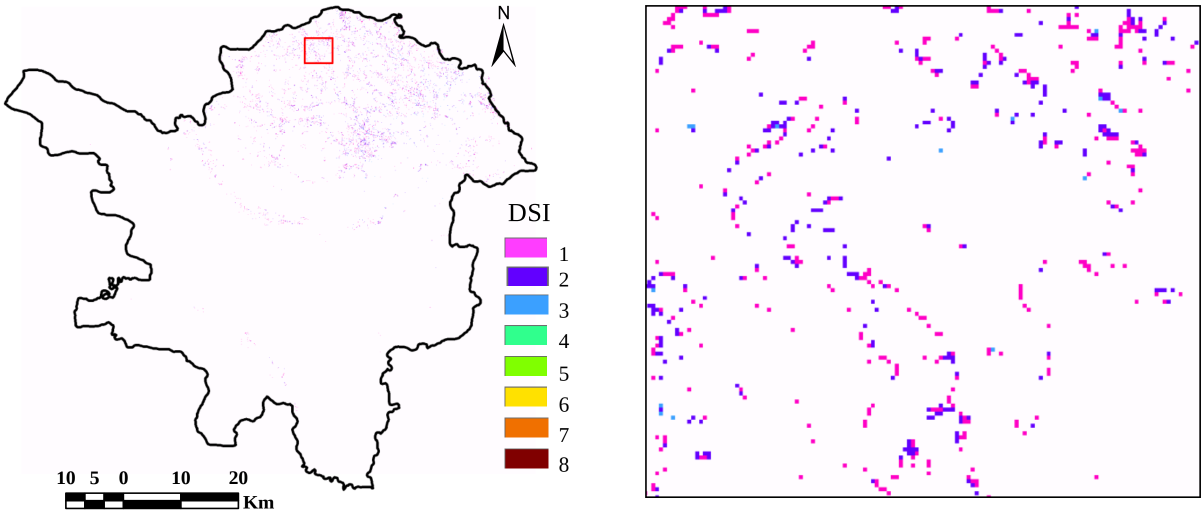
N
DSI
1
2
3
4
5
6
7
8
10 5 0 10 20
Km

(a)

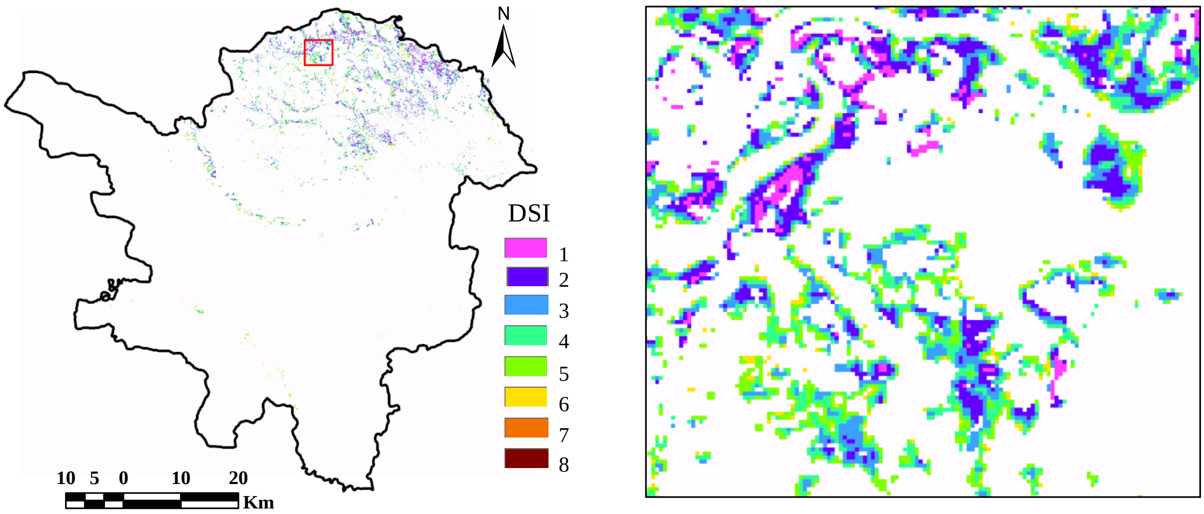
N
DSI
1
2
3
4
5
6
7
8
10 5 0 10 20
Km

(b)

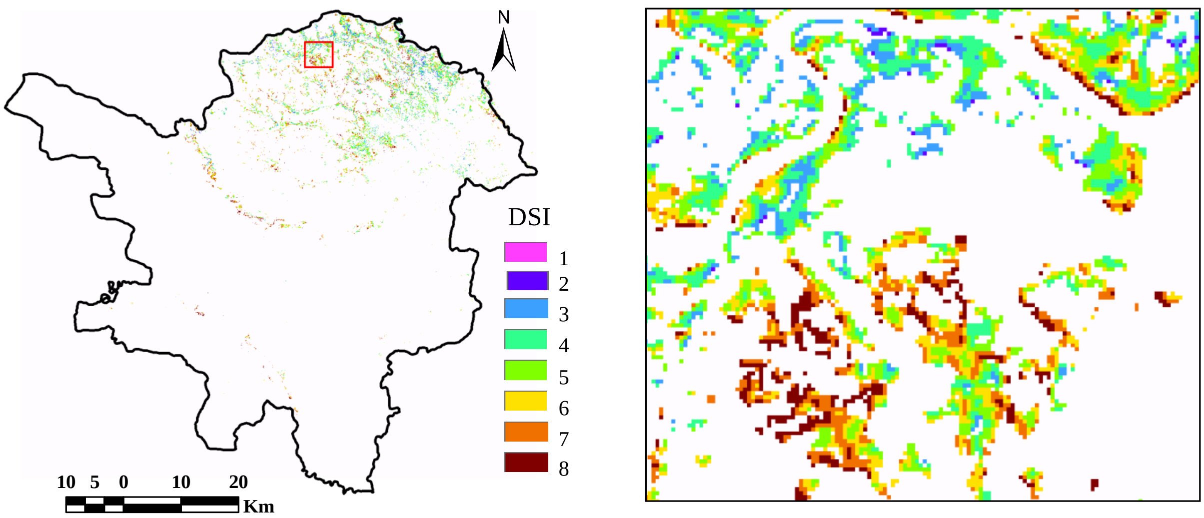
N
DSI
1
2
3
4
5
6
7
8
10 5 0 10 20
Km

(c)

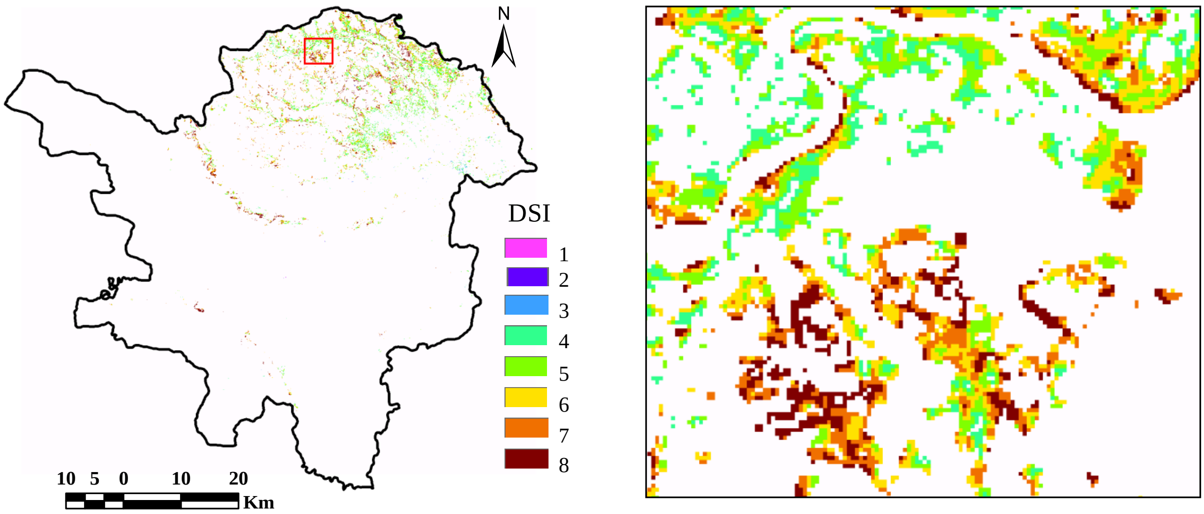

(d)

Figure 6.21: Potato Late Blight Disease Severity Over the Observation Dates in Paschim Medinipur District with Zoomed View on (a) 10th Jan 14 (b) 25th Jan 14 (c) 13th Feb 14 (d) 18th Feb 14

6.4.5 Progression and Spatial Temporal Pattern of PLB Disease

The disease severity classification maps were used to estimate the areas under different levels of disease intensity (as per DSI scale used in the study) for each satellite overpass dates. The derived data were arranged to develop spatial and temporal progress database for PLB disease. The disease spreading was assessed over 5 dates during 2012-13 and 4 dates during 2013-14 respectively in correspondence with the satellite overpass dates.

The spatial progress of disease severity as area wise estimate under different DSI values with respect to the satellite over pass days are presented in Table 6.9, 6.10, 6.11, 6.12 and 6.13 for the districts of Paschim Medinipur, Bankura, Burdwan, Hooghly and Howrah respectively. The analysis shows the areas under lower DSI (1 to 3) scale were more during initial periods of observation i.e. before 25 January in both the years.Towards later phase the areas under lower DSI scale values (1-3) were mostly zero or of very low values whereas the areas under higher DSI values progressively increased. This shows progress of disease severity only in the affected areas towards later part of growth whereas new areas were not infested after 25 January. This trend was followed in all the districts under study. The general trend also shows that the rate of spreading of infestation (increase in PLB affected area) was maximum between 15 January to 25 January. In Paschim Medinipur district there was almost 8 fold increase in total PLB affected area during this 10 days period in 2012-13, whereas in 2013-14 it was five fold increase in diseased area during similar period. Towards later part of February in both the years the disease affected area remained almost steady. Similar trend was also observed in other districts, only the spreading rate varied considerable. In Hooghly and Howrah districts in 2012-13 rapid spreading of PLB affected areas continued till 4 February.

Table 6.9: Spatial Distribution of Areas (remote sensing based) under Different Severity Classes over the Observation Dates in 2013 and 2014 in Paschim Medinipur District

Dates	PLB affected areas (ha) under different disease severity								
	DSI 1	DSI 2	DSI 3	DSI 4	DSI 5	DSI 6	DSI 7	DSI 8	Total
2012-13									
15Jan, 13	64.0	847.9	1303.3	0	0	0	0	0	2215.2
25Jan, 13	755.1	1719.7	2749.5	3459.5	3801.9	4087.9	2829.8	0	19403.3
04Feb, 13	0	0	77.8	869.3	2444.7	4303.6	9354.8	3349.1	20399.2
23Feb, 13	0	0	0	116.7	776.4	5066.3	14283.1	10826.1	31068.6
28Feb, 13	0	0	0	0.0	41.4	228.3	6123.7	24746.7	31140.1
2013-14									
15Jan, 14	3294.2	2462.3	450.1	0	0	0	0	0	6206.5
25Jan, 14	3183.9	5594.1	6685.1	7036.0	6249.9	2261.4	79.4	2.5	31092.2
13Feb, 14	0	859.2	3795.1	6888.4	7742.7	5372.1	3548.4	3147.9	31353.8
18Feb, 14	2.5	33.5	155.0	6366.5	9029.6	7053.3	4846.5	4370.4	31857.2

Table 6.10: Spatial Distribution of Areas (remote sensing based) under Different Severity Classes over the Observation Dates in 2013 and 2014 in Bankura District

Dates	PLB affected areas (ha) under different disease severity								
	DSI 1	DSI 2	DSI 3	DSI 4	DSI 5	DSI 6	DSI 7	DSI 8	Total
2012-13									
15Jan, 13	94.1	356.2	480.4	0	0	0	0	0	930.7
25Jan, 13	859.2	1503.9	1877.7	1931.7	1772.4	1717.2	1176.6	0	10838.7
04Feb, 13	0	0	60.2	555.7	1644.4	3137.1	7046.8	2647.9	15092.1
23Feb, 13	0	0	0	47.7	343.7	1959.3	8802.9	7357.9	18511.4
28Feb, 13	0	0	0	0	2.5	12.5	1481.4	16993.7	18490.1
2013-14									
15Jan, 14	2240.4	1842.4	438.9	0	0	0	0	0	4521.6
25Jan, 14	3333.9	4389.0	5094.4	5410.6	4800.6	1454.3	28.5	0	24511.2
13Feb, 14	0	445.1	2376.7	4329.5	5316.4	3529.8	3730.6	4219.1	23947.1
18Feb, 14	0	19.8	48.4	2013.5	4759.7	5383.3	3973.6	8439.5	24637.7

Table 6.11: Spatial Distribution of Areas (remote sensing based) under Different Severity Classes over the Observation Dates in 2013 and 2014 in Burdwan District

Dates	PLB affected areas (ha) under different disease severity								
	DSI 1	DSI 2	DSI 3	DSI 4	DSI 5	DSI 6	DSI 7	DSI 8	Total
2012-13									
15Jan, 13	36.4	131.7	173.1	0	0	0	0	0	341.2
25Jan, 13	385.1	1023.5	1628.1	1261.9	646.0	496.7	318.6	0.0	5759.9
04Feb, 13	0	0	11.3	207.0	962.1	2282.9	6028.3	2344.4	11835.9
23Feb, 13	0	0	7.5	195.7	777.7	2053.3	4666.1	3332.8	11033.1
28Feb, 13	0	0	0	0	3.8	31.4	1335.9	9649.6	11020.6
2013-14									
15Jan, 14	2842.9	2573.9	937.3	0	0	0	0	0	6354.1
25Jan, 14	4349.3	6171.8	6610.7	6784.3	6199.1	1931.6	136.4	0	32183.3
13Feb, 14	0	3095.8	5560.6	6646.7	6418.6	4351.8	3615.3	3279.3	32968.1
18Feb, 14	0	1.2	21.1	3549.6	7545.5	7880.3	6073.9	8342.8	33414.4

Table 6.12: Spatial Distribution of Areas (remote sensing based) under Different Severity Classes over the Observation Dates in 2013 and 2014 in Hooghly District

Dates	PLB affected areas (ha) under different disease severity								
	DSI 1	DSI 2	DSI 3	DSI 4	DSI 5	DSI 6	DSI 7	DSI 8	Total
2012-13									
15Jan, 13	0	0.9	8.5	11.6	8.2	0	0	0	29.2
25Jan, 13	49.9	104.1	125.4	96.9	69.9	63.3	42.0	0	551.6
04Feb, 13	0	0.0	62.4	920.1	2675.8	3656.7	3998.2	1268.1	12581.3
23Feb, 13	0	0.0	62.7	990.6	2276.0	2909.7	3348.1	1972.8	11559.9
28Feb, 13	0	0.0	0	0	42.0	314.2	4852.1	6355.7	11564.0
2013-14									
15Jan, 14	3419.4	2645.2	755.7	0	0	0	0	0	6820.3
25Jan, 14	5270.5	7510.2	8304.0	7603.5	5257.8	942.9	24.2	2.8	34915.8
13Feb, 14	0	2867.4	7423.1	9888.2	8893.2	4014.5	2013.8	1493.1	36593.3
18Feb, 14	0	17.4	253.2	9268.9	12520.3	7925.2	3688.2	3134.6	36807.8

Table 6.13: Spatial Distribution of Areas (remote sensing based) under Different Severity Classes over the Observation Dates in 2013 and 2014 in Howrah District

Dates	PLB affected areas (ha) under different disease severity								
	DSI 1	DSI 2	DSI 3	DSI 4	DSI 5	DSI 6	DSI 7	DSI 8	Total
2012-13									
15Jan, 13	0	3.1	2.8	0	0	0	0	0	6.0

25Jan, 13	10.4	35.1	60.2	41.4	12.2	9.1	7.5	0	175.9
04Feb, 13	0	0	0.9	46.4	208.9	550.3	887.1	316.7	2010.4
23Feb, 13	0	0	9.4	73.7	189.1	371.0	632.2	419.0	1694.3
28Feb, 13	0	0	0	0	2.8	27.0	580.4	1079.4	1689.6
2013-14									
15Jan, 14	440.5	280.5	87.1	0	0	0	0	0	808.1
25Jan, 14	188.8	398.9	702.7	963.7	875.3	196.8	4.7	0	3330.8
13Feb, 14	0	79.4	353.4	825.7	1079.6	592.0	258.8	186.9	3375.7
18Feb, 14	0	2.2	74.4	990.0	1176.9	602.9	287.0	280.2	3413.5

6.5 Conclusion

The application of multispectral remote sensing to discriminate disease affected potato crops from the healthy ones is important with respect to disease monitoring, forwarning and agroadvisory system as well as loss assessment due to PLB for the benefit of planners.

Among different multispectral vegetation indices tested in this study, NDVI was found to be the most sensitive to disease severity. For potato late blight disease discrimination NIR and SWIR bands could also be used effectively. The multiple regression using NDVI and PCCF as independent variables could be able to delineate PLB affected areas with respect to different disease severity index (DSI) values. In this study the NDVI-PCCF based model for potato late blight disease monitoring was successfully used to assess disease spreading in spatial as well as intensity scale.

However, there are several limitations in the present study. The satellite based monitoring system relies only on spectral response of crop plant to the stress induced by disease infestation. This is an indirect method and is always subject to interference by other biotic and abiotic stress factors. In field conditions there are numerous sources of vaiability like, difference in date of planting, timing of irrigation, fertilizer application as well as number of pests and disease complex (other than PLB) which must have influence on spectral properties of potato crop stand. This could add to the errors associated with the study, particularly in the event of lower disease infestation where other interfering factors predominate.

Availability of cloud/haze free satellite data during critical observation period is another important limitation of such kind of studies. Such study is executable only where cloud free satellite data with high periodicity is available for the study area in real time basis.

This approach only relied on spectral indices that describe the PLB induced crop stress. The underlying factors e.g., microclimatic factors, plant moisture potential, leaf wetness duration atmospheric humidity, fog duration etc. that could cause the PLB development have not been studied. Hence this study is not highly effective as a disease forewarning and agroadvisory system.

Besides all limitations, this opens the scope for further research incorporating microwave remote sensing components that could derive valuable information about moisture regime, canopy density as well as microclimatic variables. Different numerical and rule based models can also be implemented using satellite derived input variables for development of a forwarning system, that can have far reaching implication in potato growing regions.